Scientific Research Publishing

Advances in Biological Chemistry, 2026, 16(6), 85-117
https://www.scirp.org/journal/abc
ISSN Online: 2162-2191
ISSN Print: 2162-2183

A Systematic Study on the Influence of Essential Oils as Promoter of Changes on Physicochemical and Antimicrobial Characteristics of Poly (Butylene Adipate-Co-Terephthalate) Composites

Isabella Carneiro Gonçalves[1], Enzo Erbisti Garcia[1], Gerson Alberto Valencia Albitres[1], Eduardo Moreira Silva[2], Agnes Maria Cupertino Fernandes Araújo[3], Marco Antônio Lemos Miguel[3], Michelle Gonçalves Mothé[4], Luis Claudio Mendes[1]

[1]Instituto de Macromoléculas Professora Eloisa Mano, Universidade Federal do Rio de Janeiro, Centro de Tecnologia, Rio de Janeiro, Brazil
[2]Faculdade de Odontologia, Universidade Federal Fluminense, Niterói, Brazil
[3]Instituto de Microbiologia Paulo de Góes, Federal Universidade Federal do Rio de Janeiro, Rio de Janeiro, Brazil
[4]Escola de Química, Universidade Federal do Rio de Janeiro, Centro de Tecnologia, Bloco J, Rio de Janeiro, Brazil
Email: isabellacg@ima.ufrj.br, lcmendes@ima.ufrj.br

How to cite this paper: Gonçalves, I.C., Garcia, E.E., Albitres, G.A.V., Silva, E.M., Araújo, A.M.C.F., Miguel, M.A.L., Mothé, M.G. and Mendes, L.C. (2026) A Systematic Study on the Influence of Essential Oils as Promoter of Changes on Physicochemical and Antimicrobial Characteristics of Poly (Butylene Adipate-Co-Terephthalate) Composites. *Advances in Biological Chemistry*, **16**, 85-117.
https://doi.org/10.4236/abc.2026.166007

Received: October 29, 2026
Accepted: November 17, 2026
Published: November 20, 2026

Copyright © 2026 by author(s) and Scientific Research Publishing Inc.
This work is licensed under the Creative Commons Attribution International License (CC BY 4.0).
http://creativecommons.org/licenses/by/4.0/

Open Access

Abstract

Essential oils are sustainable substances with properties that enable their application in fields ranging from human health to technology. This study investigated the addition of different essential oils, singly and in mixtures, into a poly(butylene adipate-co-terephthalate) (PBAT) matrix. Rosemary, cinnamon, clove, thyme and a blend of cinnamon/clove/thyme were tested and their effects on the physicochemical and antimicrobial characteristics were assessed. DRX revealed the influence of phosphate and type of essential oil on the PBAT crystalline arrangement. Spin-lattice and spin-spin relaxations showed that molecular mobility of PBAT was dependent on the type of essential. By thermogravimetry, PBAT thermal stability was slightly affected by the presence of oil and phosphate. Crystallization and melting temperature changed according to the type of PBAT composite but the degree of crystallinity was reduced for all samples. Antimicrobial activity was evaluated against Gram-positive and Gram-negative bacteria, fungi and yeast showing tremendous effectiveness. The mixing of clove, cinnamon and thyme oils showed remarkable effect against oral bacteria such as Enterococcus faecalis and Lactobacillus acidophilus.

Keywords

Rosemary Oil, Clove Oil, Cinnamon Oil, Thyme Oil, PBAT

1. Introduction

The development of biodegradable polymeric materials with functional properties has sparked interest across various fields, primarily due to the potential to combine the characteristics of the polymer matrix with the activity of bioactive compounds. In this context, poly(butylene adipate-co-terephthalate) (PBAT), derived from fossil sources, stands out among biodegradable polymers for its flexibility and properties suitable for film production. Incorporating active substances into it expands its potential applications, particularly when the goal is to produce materials with new functionality. Films of PBAT embedded with thyme essential oil (0, 1, 2, 5, 10, 15, and 20 wt.%) were studied by Luna *et al.* [1]. The authors reported that thyme essential oil offered effectiveness against both gram-positive and gram-negative bacteria and that mechanical and thermal properties were dependent on the oil concentration. A nano hybrid filler of titanium oxide/tannic acid TiO_2-TA (TiTA) was added to PBAT matrix. Composite PBAT/TiTA (92.5/7.5 wt./wt.%) revealed notable mechanical and thermal decomposition as well as easy biodegradability by cutinase enzymatic degradation [2]. As a nucleating agent, potassium dimethyl 5-sulfoisophthalate was added to the composites based on PBAT and recycled carbon fiber. Markedly, the improvement on crystallization behavior, increasing crystallization temperature, crystallization rate and crystallinity was registered [3]. Lignin (1 and 3 wt.%) was added to PBAT in order to assess composting conditions using weight loss and mineralization rate. It was registered that for 40 days the composite with 1 wt.% of lignin showed hydrolytic weight loss of 18.3% while the other one lose 28.6%. The authors pointed out that appropriate lignin loading enables balanced performance and degradation controllability, offering new insights into lifecycle assessment of green composites [4]. Composites of PBAT with chitosan (10, 20, 30 wt.%) were studied by Sarmin *et al.* Tensile strength, elongation at break and thermal properties decreased while storage modulus increased. According to them, infrared suggested intermolecular interactions between PBAT and chitosan through hydroxyl and carbonyl functional groups [5]. Sulfonic acid-based ionic liquid ([TBP]TS), ammonium polyphosphate (APP) and boron nitride (BN) were incorporated into poly (lactic acid) PLA/PBAT polymer blend. The ionic liquid promoted improvement in the interfacial region of the polymer blend meaning compatibility besides increases in the flame retardancy and mechanical properties [6]. A study on the influence of various cellulosic fillers with different sizes, aspect ratios, and contents on composites of PBAT was performed by Keskes *et al.* All fillers showed a nucleating effect on PBAT crystallization. Low aspect ratio fillers preserved elongation at break, providing moderate stiffness enhancement

and reasonable ductility [7]. Silanized cellulose (SC) was added to PBAT. Microstructural evaluations revealed that SC had a role as a heterogeneous nucleating agent and increased the crystallization temperature but owing to its steric hindrance PBAT crystal growth was suppressed [8]. Essential oils have garnered attention in this regard because they contain compounds capable of acting against various microorganisms. Notable examples include clove, cinnamon, thyme, and rosemary oils, which contain constituents such as eugenol, cinnamaldehyde, thymol, and carvacrol compounds associated with distinct antimicrobial mechanisms. Studies have demonstrated the activity of these compounds against microorganisms of human health significance, including species involved in biofilm formation [9] [10]. Incorporating essential oils into polymer films has also yielded promising results. Tian *et al.* [11] developed PBAT/thermoplastic starch films containing cinnamon essential oil and observed antibacterial activity against *Escherichia coli, Staphylococcus aureus, and Shewanella putrefaciens*. The authors also found that the matrix composition influenced oil retention and release, demonstrating a direct link between these characteristics and the film's antimicrobial activity. Beyond the interest in producing antimicrobial films, these oils are particularly relevant to dentistry. Dental caries and other oral diseases are linked to biofilm formation, and various studies have investigated the use of natural compounds as an alternative strategy for controlling these microorganisms. Cinnamon essential oil, for instance, exhibits activity against various oral pathogens, while eugenol, the main component of clove oil, has demonstrated antibacterial and antibiofilm activity against *Porphyromonas gingivalis,* a key microorganism associated with periodontal disease [12] [13]. Similar results have been observed for clove, thyme, and cinnamon essential oils in studies focused on controlling cariogenic microorganisms. Carvalho *et al.* verified the antibacterial activity of these oils against various species found in the oral cavity, as well as their effect on *Streptococcus mutans* biofilms. A systematic review also highlighted the potential of various essential oils, including those of interest to dentistry, in controlling bacteria associated with dental caries [14]. Given this evidence, incorporating clove, cinnamon, thyme, and rosemary essential oils into PBAT films represents a promising approach for developing biodegradable materials with antimicrobial activity. Combining a polymer matrix with naturally derived bioactive compounds can yield functional films with potential for applications where microbial control is crucial, including future uses in biomedical and dental systems. However, applications involving direct contact with the body require specific studies on biocompatibility, cytotoxicity, and the release of the active compounds. Kannan & Girija evaluated the antibacterial and antibiofilm efficacy of eugenol against clinical isolates of Enterococcus faecalis in persistent root canal infections. Eugenol revealed great antibacterial and antibiofilm activity against *E. faecalis*. Computational analyses indicated potential interactions with virulence-associated proteins involved in important metabolic pathways [15]. Dewi *et al.* investigated the action of ethanol extract of bay leaves as antibacterial and antibiofilm against

Streptococcus sanguinis and *Streptococcus mutans* bacteria. The authors concluded that bay leaf extract was effective for both purposes but revealed a stronger antibiofilm effect than its antibacterial effect [16]. Akbar *et al.* investigated the prevention of dental plaque formation by isolating dental plaque bacteria and using plant extract (clove-Syzygium aromaticum) against it. Remarkable antibacterial activity with zone of inhibition between 8mm to 20mm in 1 mg/disc was achieved [17]. Zainal-Abidin evaluated the effectiveness of Halia Bentong (Zingiber officinale Roscoe) against *Porphyromonas gingivalis*. The extract of Halia Bentong inhibited the growth of *P. gingivalis* by concentration-dependent manner, while anti-adhesion activity was inversely dependent on concentration. SEM images revealed surface changes and reduced cell numbers when compared with untreated samples [18]. Zhang *et al.* ascertained the action of eugenol extracted from leaf essential oil against periodontal pathogen *Porphyromonas gingivalis*. Eugenol showed antibacterial activity against *P. gingivalis* at a concentration of 31.25 μM. Scanning electron microscopy revealed cell shrinkage and lysis caused by eugenol. The release of macromolecules and uptake of fluorescent dye indicated that the antibacterial activity was due to the ability of eugenol to permeabilize the cell membrane and destroy the integrity of the plasmatic membrane irreversibly. In addition, eugenol inhibited biofilm formation and reduced preformed biofilm of *P. gingivalis* at different concentrations [13]. A systematic evaluation of rosemary, cinnamon, clove, thyme and mixing of cinnamon/clove/thyme essential oils on the physicochemical and antimicrobial properties of singly PBAT and in composites containing titanium phosphate (LTiP) was performed. The designed interactions among polymer/oil, polymer/LTiP and LTiP/oil are overlaid on the relaxation time, thermal stability, crystallization/melting temperatures and antimicrobial activity.

2. Experimental

2.1. Materials

Table 1. Cinnamon, clove, rosemary, and thyme oils and their characteristics.

Essential oil	Main constituent	Other important constituent	Oil composition (%)
Rosemary (*Salvia rosmarinus*, sin. Rosmarinus officinalis)	1,8-cineole (eucalyptol)	Camphor, *α*-pinene, *β*-pinene e camphene	1,8-cineole: 40.10%; *α*-pinene: 12.94%; camphor: 12.40%; *β*-pinene: 8.94%; canphene: 6.38% [19]
Clove (*Syzygium aromaticum*)	Eugenol	*β*-cariophyllene, eugenyl acetate	Eugenol: 76.08%; eugenyl acetate: 12.57%; *β*-cariophyllene: 9.98% [20].
Cinnamon (Cinnamomum spp.)	Cinamaldehyde	Eugenol, *β*-cariophyllene	Cinamaldehyde: 54.5%; eugenol: 10.2%; *β*-cariophyllene: 6.0% [21].
Thyme (*Thymus vulgaris*)	Thymol or carvacrol, depending on the chemotype	p-cymene, *γ*-terpinene, linalool	Thymol: 35.1%; p-cymene: 31.6%; carvacrol: 0.87% [22].

Titanium isopropoxide ($C_{12}H_{28}O_4Ti$), phosphoric acid (H_3PO_4 85% w/w), ethanol (C_2H_6O, 99%), chloroform ($CHCl_3$) were purchased from Sigma-Aldrich Ltd. Poly(butylene adipateterephthalate) (PBAT Ecoflex® F Blend C 1200) was supplies from BASF S.E. and the essential oils Rosemary (*Rosmarinus offinalis*) from Phytoterápica, Cinnamon from Phytotratha Cosmeticos Ltda, Clove (*Eugenia caryophyllus*) and White Thyme (*Thymus vulgaris*) from RHR Rivera. In Table 1 below, the main constituents of the essential oils used in this study, along with their reference percentages, can be observed.

2.2. Synthesis of LTiP

For the synthesis of LTiP, 1.15 mL of titanium isopropoxide and 0.35 mL of phosphoric acid (85%) were added to 10 mL of analytical-grade ethanol, and the mixture was kept under constant stirring for 10 minutes. After this period, an ethanol washing step was performed, consisting of three successive cycles. In each cycle, the supernatant was removed and discarded; subsequently, ethanol was added to the remaining material, and the system was kept under stirring, with a 10-minute interval between each wash. Upon completion of the three washing steps, 38.7 mL of ethanol was added to the suspension, and the system was kept under constant stirring for 72 hours at room temperature to complete the LTiP synthesis process.

2.3. Composites Preparation (PBAT/TiP/EO Films)

4.0 g of PBAT was added to 15 mL of chloroform, and the mixture was kept at 25˚C under constant stirring for 30 minutes until a homogeneous solution was obtained. Concurrently, an LTiP solution was prepared by dispersing 0.08 g of the material in 10 mL of chloroform at 25˚C under stirring for 20 minutes. Next, this solution was added dropwise to the PBAT solution while maintaining stirring throughout the process. Subsequently, 2.0 g of each essential oil evaluated—rosemary (RO), clove (CLO), cinnamon (CiO), and thyme (TO)—as well as a mixture of clove, cinnamon, and thyme essential oils in a 1:1:1 ratio, were added dropwise. After the addition of the essential oils, the solutions were kept at room temperature (25˚C) under constant stirring for 24 hours to ensure proper homogenization of the components. At the end of this period, the solutions were poured into Petri dishes and kept at room temperature (25˚C) to allow for solvent evaporation and subsequent film formation. For all composites, their composition was PBAT/LTiP/Oil—65.7/1.3/33.0 wt./wt./wt.%. The samples were labeled as following: PBAT-LTiP-RO, PBAT-LTiP-CLO, PBAT-LTiP-CiO, PBAT-LTiP-TO and PBAT-LTiP-CLCiTO.

2.4. Infrared Spectroscopy

Fourier-transform infrared spectroscopy (FTIR) was performed using a Perkin Elmer Frontier equipment in the range of 4000 - 500 cm^{-1}, with 120 scans and a resolution of 4 cm^{-1}.

2.5. X-Ray Diffraction

The crystallographic structure was evaluated using a wide-angle X-ray diffractometer Rigaku Miniflex, employing CuKα radiation with a wavelength λ = 1.5418 Å, a Ni filter, a current of 20 mA, a voltage of 20 kV, 2θ between 2˚ - 60˚ and resolution of 0.05˚.

2.6. Time Domain Nuclear Magnetic Resonance

The application of a magnetic field in the study of molecular motions is considered a powerful technique to evaluate relaxation times. Different nuclear magnetic resonance processes named longitudinal and transverse relaxation times allow access to the molecular mobility of polymers, fluids, and so on. Herein, longitudinal magnetization (T_1) and transverse magnetization (T_2) were applied to evaluate the effect of fillers on the polymer molecular motion. Time domain nuclear magnetic resonance was performed using a MARAN Ultra 0.54 T (23.4 MHz for ^{1}H) equipment, with a probe diameter of 18 mm and WinFit 2.4-point adjustment software. Evaluation of longitudinal relaxation time (T_1)—also known as spin-lattice relaxation time—of PBAT and composites represents the result of the existence of transient magnetic moments produced by the rotational and translational movements of neighboring molecules. T_1 was measured by an inversion-recovery pulse sequence (recycle delay −180˚, τ – 90˚ - acquisition data), 90˚ pulse of 7.5 μs, automatically calibrated by equipment software. Molecular relaxation of PBAT and composites was performed by transverse relaxation time (T_2) using magic sandwich echo-free induction decay (MSE-FID). The analysis was performed at a temperature of 30˚C ± 2˚C, with a 2-Eco-Solid pulse sequence, a pulse duration of 90˚ in 7.5 μs, with 2048 points spaced 0.5 μs apart. The number of accumulations corresponds to 64, with a recycling time of 1 second and a receiver gain of 8%. The adjustment function for the MSE-FID signals was determined by Equation (1): A_R: amplitude or fraction of the rigid region; A_M: amplitude or fraction of the moving region; T_2*: transverse relaxation time of each of the fractions obtained by the equipment; μ_b: centroid of the Gaussian function; K: offset or baseline of the relaxation signal that compensates for the influence of noise during nonlinear tuning. The signal is governed by two components. The first (on the left) is related to highly rigid ^{1}H nuclei and is governed by a Gaussian function. The second (on the right) is characterized by more mobile hydrogens that exhibit higher T_2 values and an exponential decay. The fraction corresponding to each domain was calculated according to Equation (2), where (A_R) represents the area of the rigid domain, (A_M) the area of the mobile domain, and (Ax) the area of the domain of interest, for which the relative fraction was determinated.

Equation (1):

$$A(t) = A_R \exp\left[-\left(\frac{\tau - \mu_b}{2T_{2+R}}\right)^2\right] + A_M \exp\left[-\left(\frac{\tau}{T_{2+M}}\right)\right] + K$$

Equation (2):

$$X(\%) = \frac{A_x}{(A_R + A_M)} \times 100$$

2.7. Thermogravimetry

Samples thermal stability was conducted in a TA Instruments Q-500 equipment, in the range of 25˚C - 700˚C, at 10˚C/min, in a nitrogen atmosphere. T_{onset}, T_{10}, T_{max} and residue were evaluated.

2.8. Differential Scanning Calorimetry

Differential scanning calorimetry was performed using a TA Instrument Q1000 model. Two heating routes (first and third cycles, 10˚C - 190˚C, 10˚C/min) and one cooling (second cycle) were performed Crystallization and melting temperatures (T_c and T_m) were taken. The degree of crystallinity (X_c) was determined based on the ratio of the experimental melting enthalpy to the melting enthalpy of 100% crystalline PBAT (114 J/g) [23].

2.9. Scanning Electron Microscopy (SEM) and Etching Procedure

SEM images were captured using a Tescan field emission microscope, model MIRA 4 LMU (LowVac Mode UniVac™) equipment, voltage of 10 kV. For etching procedure, a small piece of each film composite was weighed before and after exposure to ethanol vapor. The sample was attached to the stopper of an Erlenmeyer flask, and 10 mL of ethanol was added to the bottom of the flask, sealed/isolated for 7 days. After that, the sample was removed from the apparatus, dried and weighed. The mass loss was considered the difference between before and after etching. Then, each sample was submitted to SEM analysis and the surface was compared before and after the etching process.

2.10. Microbiological Evaluation

Origin and preparation of microorganisms: Gram-positive and Gram-negative bacteria were used which differ due to the chemical composition of the cell wall. As Gram-negative bacteria were tested, *Escherichia coli* from American Type Culture Collection (ATCC) 11229, *Salmonella Enteritidis* 13076 and *Pseudomonas aeruginosa* ATCC 15442. Gram-positive bacteria tested were *Staphylococccus aureus* ATCC 29213, Listeria monocytogenes ATCC 19117, *Bacillus cereus* ATCC 14579, *Enterococcus faecalis* ATCC 19433 and *Lactobacillus acidophilus* NCFM (ATCC SD5221). The Yeast (fungus) Candida albicans ATCC 10231 was also included. All microorganisms belonged to the culture collection of the Institute of Microbiology Paulo de Góes at UFRJ. These microorganisms were selected due to their frequent involvement in clinical infections or foodborne diseases in humans. The microorganisms were stored under refrigeration and were activated for the experiments. The bacteria were activated by cultivation in 5 ml of liquid culture medium—Brain Heart Infusion (BHI-Merck) for 24 h. Candida albicans were propagated in Saboraud Broth (Merck) for 48 h. Both bacteria and yeast were in-

cubated at 37˚C. After activation, the strains were streaked across the surface on BHI agar (Merck) and Saboraud agar (Merck) plates and incubated at 37˚C to obtain isolated colonies. From each microorganism, approximately 5 colonies were used to prepare a suspension in sodium chloride solution 0.85% (w/v) to reach a cell concentration of approximately 108 colony-forming units per milliliter (CFU/ml). From the suspensions, microorganisms were inoculated directly onto the surface of BHI agar or Saboraud agar plates, for bacteria and yeast, respectively. The inoculum was made with a sterile swab (wooden rod with cotton tip) in 3 different directions, to achieve confluent microbial growth. Disks of 6 mm were carefully placed on the agar surface under aseptic conditions. The inoculated plates were incubated at 37˚C, for 48 h. Antibacterial activity was assessed by measuring the zone of inhibition (mm) against each test organism. All experiments, including antimicrobial activity assays, were conducted in triplicate using three independently prepared film samples (n = 3).

3. Results and Discussion

3.1. Fourier Transform Infrared Spectroscopy (FTIR)

Figure 1 presents the infrared spectra of the samples. FTIR spectra show that the incorporation of LTiP and the essential oils of rosemary (RO), clove (CLO), cinnamon (CiO), and thyme (TO), as well as the CLCiTO mixture, did not significantly alter the main chemical structure of PBAT. The PABT main bands are present in all samples, although some differences in intensity and shape are observed, particularly in the fingerprint region. Table 2 compiles band absorptions and attributions for all samples. The most intense band, located around 1710 cm^{-1}, is associated with the C=O stretching of the PBAT ester groups. Its presence in all samples indicates the preservation of the copolyester structure even following the incorporation of the different components. PBAT bands near 2950 - 2850 cm^{-1}, related to the C-H stretching of aliphatic groups, and around 1265, 1170, and 1100 cm^{-1}, attributed primarily to the C-O and C-O-C vibrations of the ester groups also were seen [24]. The most significant differences between the formulations appear between approximately 1300 and 700 cm^{-1}; this region is particularly important as it encompasses both the PBAT bands and the contributions from the essential oils. In the composite containing rosemary oil (RO), these changes may be associated with the presence of 1,8-cineole, which has been reported in the literature to exhibit characteristic absorption bands near 1214, 1080, and 985 cm^{-1}. For clove oil (CLO), the main constituent, eugenol, may contribute to the absorption bands associated with aromatic structures and C-O-C bonds, particularly in the 1500 - 1100 cm^{-1} region, as reported in the literature [25] [26]. In the case of cinnamon oil (CiO), the presence of cinnamaldehyde may be associated with absorption bands in the region near 1680 - 1700 cm^{-1}, corresponding to its conjugated carbonyl group, as reported in the literature. Furthermore, this region also encompasses the strong carbonyl absorption band of PBAT, suggesting that overlapping signals may occur.

As for thyme oil (TO), its main constituents, thymol, carvacrol, and p-cymene, may contribute to the absorption bands observed near 1516, 1419, 1289, 1154, 945, and 813 cm^{-1}, as reported in the literature [26]. Combining LTiP-ClCiTO with PBAT results in greater likelihood of overlapping between the characteristic bands of these components and those of PBAT. Overall, the absorption bands observed in the PBAT structure contain aliphatic and aromatic linkages such as C-C, C-H, C-O, C=O bonds. These bands are also present in the chemical structure of the main components found in essential oils. It is difficult to find differences in the spectra owing to the overlapping of the majority of bands.

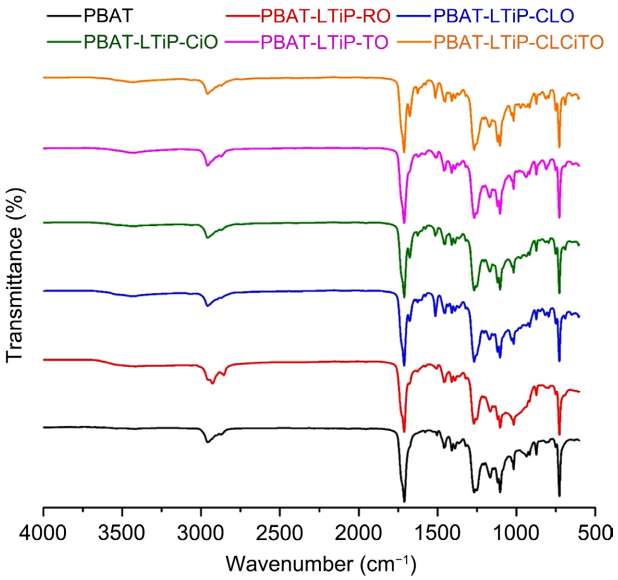

Figure 1. Samples infrared spectra.

Table 2. Compilation of the samples infrared absorptions and attributions.

Samples	Absorptions (cm^{-1})	Band assignment	References
PBAT	**2950, 1710, 1460, ~1260, ~1170 - 1100, ~870 - 800, ~730 - 720**	(C-H) stretching of aliphatic CH_2/CH_3 groups, (C=O) stretching of ester groups (main characteristic band), CH_2/C-H bending vibrations, (C-O) stretching (important polyester band), (C-O-C)/C-O stretching of PBAT ester groups, Out-of-plane C-H bending of the aromatic ring, CH_2 bending/aromatic C-H bending.	[1]
LTiP	**~3500 - 3000, 1640 - 1620, ~1250 - 1200, ~1120 - 1000, ~970 - 900, ~750 - 720, 630 - 615, ~550 - 400**	(O-H), P-OH and adsorbed water, (O-H) of water, P-O-H/P-OH, (P-O), PO_4 and Ti-O-P, P-O-P/P-O, P-O/Ti-O-P, Ti-O-P, (O-P-O), Ti-O and PO_4	[27] [28]
PBAT-LTiP-CiO	~1710, 1625 - 1600, ~1260 - 1200, ~1100 - 1000	C=O of PBAT ~1680 cm^{-1} of cinnamaldehyde, C=C of cinnamon + O-H of water/TiP, C-O of PBAT + P-OH + cinnamon components, C-O/C-O-C + P-O/Ti-O-P.	[29] [30]
PBAT-LTiP-RO	~1710, ~1450, ~1275 - 1260, ~1100 - 1000	C=O of PBAT, PBAT + rosemary components, C-O of PBAT + oxygenated rosemary compounds, PBAT/TiP + C-O of rosemary.	[31] [32]

Continued

PBAT-LTiP-CLO	~1710, ~1514, ~1385 - 1247, ~1030	C=O of PBAT, aromatic C=C of eugenol, CH_2 + C-O of eugenol, C-O-C of eugenol + TiP/PBAT.	[33] [34]
PBAT-LTiP-TO	~1710, ~1580 - 1460, ~1400 - 1360, ~1250 - 1000	C=O of PBAT, aromatic bands of thymol/carvacrol, CH_3/isopropyl, PBAT + TiP + C-O of phenolic compounds.	[1] [26]
PBAT-LTiP-CLCiTO	~1710, ~1625 - 1580, ~1514 - 1450, ~1250 - 1000, ~800 - 700	C=O of PBAT + C=O of cinnamon, C=C of cinnamon + aromatic bands of thyme, aromatic C=C/eugenol + aromatic bands of the other oils, PBAT + TiP + C-O of the three oils, PBAT + aromatic bands of the oils.	[1] [27] [31] [35]

3.2. Wide-Angle X-Ray Diffractometry

Figure 2 presents the samples' diffraction patterns. Overall, the samples maintained a diffraction profile similar to that of the PBAT matrix, with the main 2θ diffraction angle around 15˚ - 26˚. Singly PBAT exhibited 2θ diffraction angles around 16.0˚, 17.0˚, 20.5˚ and 23.8˚. Aversa & Barletta on their study on compostable materials based on a blend of PBAT, poly(lactic acid) and thermoplastic starch described PBAT reflections at 16.6 (011), 17.4 (010), 20.0 (110), 23.8 (100) and 25.7 (111) which corroborates with Fukushima *et al.* study on PBAT composites filled with different clays [36]-[38]. It must be emphasized that PBAT exhibits a slow rate of crystallization which results in low overall crystallinity and a broad crystallization window as pointed out by Zhou *et al.* in an article on the enhancement of PBAT crystallization by a self-assembly nucleation agent [39]. In the composites containing essential oils, although the diffraction patterns were similar, some changes were observed. For composite PBAT-LTiP-RO, reflections at approximately at 18.0˚, 21.0˚ and 24˚ were seen. These diffraction peaks are consistent with (010), (110) and (100) PBAT crystallographic planes as described by Li *et al.* in their work on nano-lignin reinforced PBAT [40]. With the addition of LTiP, according to Schmutz *et al.*, slurry titanium phosphate forms an amorphous material without defined crystalline reflections [41]. The diffraction patterns of PBAT-LTiP-CLO and PBAT-LTiP-CiO composites resemble those of the one with rosemary oil. Araujo *et al.* studied the addition of lamellar zirconium phosphate, as synthesized and pre-intercalated with amine, and clove oil into PBAT matrix. It was pointed out that clove oil provoked the delamination/exfoliation of ZrP and both altered the crystallization process of PBAT [42]. Freitas *et al.* investigated the influence of cinnamon oil (0, 5 and 10 wt.%) in composites based on PBAT and lamellar zirconium phosphate. Mutual interaction among polymer, filler and cinnamon oil played a role in the phosphate delamination/exfoliation and the interaction between PBAT and the oil was directly related to its amount [43]. Diffraction angles of PBAT-LTiP-TO showed a relevant resemblance with PBAT around 17.0, 18.0, 20.0, 24.0 (higher intensity one) and 26.0˚. Thyme oil presented a behavior uneven with respect to their counterparts meaning that although the main crystalline structure is maintained, differences in the extent and distribution

of crystalline regions may occur. The PBAT-LTiP-CLCiTO contains a mixture of clove, cinnamon and thyme oils. Its behavior was quite similar to singly thyme but the diffraction angle around 17.0˚ - 18.0˚ was the more prominent. Li *et al.* identified reflections at 16.3˚, 17.7˚, 20.9˚, 23.6˚, and 25.5˚, demonstrating that variations in peak positions can occur without the loss of the characteristic PBAT crystalline structure. These small differences may be associated with changes in chain packing and the spacing between crystalline planes [40]. Overall, the diffractograms show that the incorporation of LTiP and the essential oils did not cause a significant alteration to the characteristic crystalline structure of PBAT. The matrix's main reflections remained present in all formulations, although differences in the intensity and position of certain reflections were observed. These changes indicated that both LTiP and oils can influence chain organization during film formation and, consequently, the development of crystalline regions.

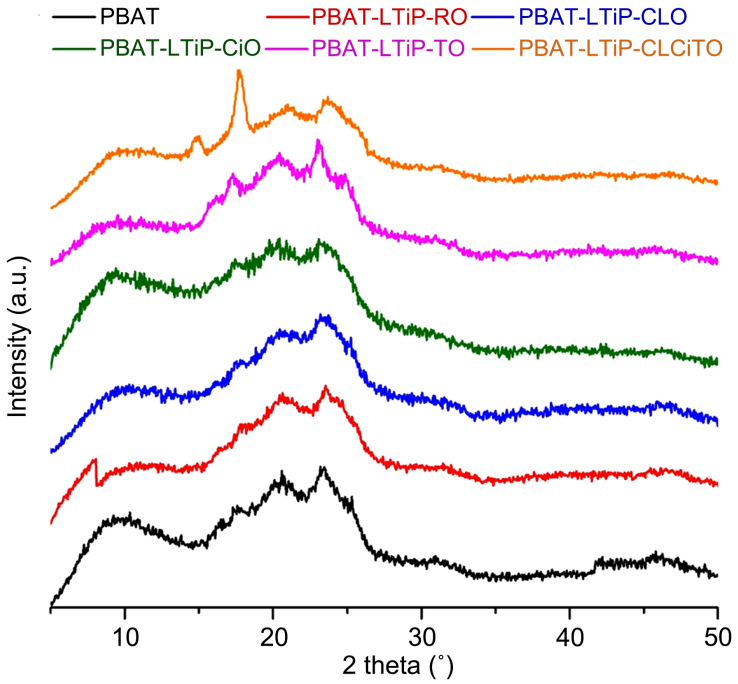

Figure 2. Diffraction patterns of the samples.

3.3. Time-Domain Nuclear Magnetic Resonance

Time-domain nuclear magnetic resonance (TDNMR) relaxometry is a useful tool for assessing molecular dynamics in polymeric materials. This technique enables the observation of differences in chain mobility, the distribution of molecular environments, and structural changes resulting from the presence of components incorporated into the matrix. These characteristics can be evaluated through hydrogen nucleus relaxation times, primarily longitudinal (T_1) and transverse (T_2) relaxation times. It is important to note, however, that these parameters should not be interpreted in isolation as direct indicators of crystallinity or miscibility, since the values obtained are influenced by molecular mobility, interactions be-

tween nuclei, and the conditions employed during analysis [44]. Herein, T_1 measurements were obtained at 30˚C ± 2˚C using the inversion-recovery sequence, with acquisition times ranging from 1 to 10,000 ms. Plotting normalized amplitude against relaxation time allows for a comparison of the response of additive-free PBAT with that observed for composites with LTiP and essential oils. Thus, differences between the curves can serve as an indicator of changes in the molecular dynamics of the polymer matrix following the incorporation of these components. **Figure 3** displays the T_1 domain curves of PBAT and composites. **Table 3** compiles the relaxation data from domain curves. For PBAT, the domain curve profile indicated that the polymer-polymer interactions are homogeneous and that there is a prevalence of a domain, consisting probably of amorphous chains. For PBAT-LTiP-RO, there was a broadening of the domain curve, and T_1 was slightly shifted to a higher value. Although the addition of LTiP-RO did not cause a very pronounced change in the matrix's predominant relaxation dynamics, the increase in T_1 is likely related to the presence of LTiP, signifying reduced molecular mobility while the broadening of the domain curve could be associated with modifications involving a combination of polymer-polymer, polymer-filler, and polymer-oil interactions. The behavior observed for PBAT-LTiP-CLO was somewhat more complex. In addition to the main domain, situated approximately between 9 and 360 ms and associated with a T_1 of 54.4 ms, a second domain was identified within a very short time range, between approximately 0.5 and 2.3 ms. The value of 54.4 ms obtained for the main domain of PBAT-LTiP-CLO is quite close to that determined for pure PBAT. Thus, the major signal contribution continues to exhibit relaxation behavior similar to that of the matrix. In contrast, the domain observed at much shorter times may be associated with a proton population subject to lesser motional restriction or a distinct molecular environment. The presence of more than one relaxation contribution may indicate the existence of molecular environments with different mobilities. This interpretation is consistent with relaxometry studies applied to multiphase polymer systems, in which different proton populations can exhibit distinct relaxation times depending on their respective mobilities and local interactions. A green and multifunctional composite based on PBAT filled with zirconium phosphate and clove oil was studied. The authors pointed out that the molecular mobility of PBAT increased with the presence of phosphates and clove oil [42]. PBAT-LTiP-CiO exhibited an even more pronounced characteristic of heterogeneity, with two T_1 values: 16.5 ms and 72.0 ms. The existence of these two domains indicates that the system does not possess a single proton population with uniform relaxation behavior. The 16.5 ms component corresponds to a population exhibiting faster relaxation, whereas the 72.0 ms domain is associated with a contribution characterized by slower relaxation. In polymeric materials, the presence of different relaxation times may be linked to the coexistence of domains with varying degrees of molecular mobility generally associated to contribution of the amorphous and crystalline portions. Clearly, the splitting of T_1 into two values, representing higher and lower molec-

ular mobility, could be related to changes in polymer-polymer interactions modified by the new polymer-filler and polymer-oil interactions. A study involving the effect of adding ZrP, both synthesized and modified with amine, along with cinnamon oil, indicated that the change in the molecular relaxation of PBAT was dependent on the type of phosphate [43]. The composite containing thyme essential oil (PBAT-LTiP-TO) differed the most from that of PBAT. For the main domain, a T_1 attained value of 96.9 ms, which is approximately 85% higher than that for PBAT. This increase indicates a significant change in the material's relaxation behavior. Since T_1 is sensitive to molecular dynamics, the observed change suggests a significant change in the composite molecular environments. Polymer studies show that changes in polymer-polymer interactions can modify relaxation times, with NMR being particularly useful for monitoring these changes as pointed out by [44] [45]. In addition to the main domain, PBAT-LTiP-TO exhibited a second domain around 1500 - 3500 ms. This domain lies far outside the predominant relaxation range observed in the other samples. The presence of this contribution may indicate a proton population with dynamics considerably different from those associated with the polymer matrix. However, given that the system contains PBAT, LTiP, and essential oil, it is not possible to identify effectively the origin of this population but it is possible to infer that new interaction(s) polymer-filler and polymer-oil emerged. For PBAT-LTiP-CLCiTO composite, a T_1 value of 48.7 ms was obtained. This value is lower than the 52.3 ms determined for PBAT, indicating a change in the matrix's relaxation behavior. The reduction in T_1 may be associated with changes in local proton dynamics and the distribution of molecular environments. However, it is important not to interpret this decrease in isolation as an increase or reduction in the polymer's overall mobility. Relaxation behavior results from a combination of different molecular motions and local interactions, particularly in materials composed of more than one component [44] [45].

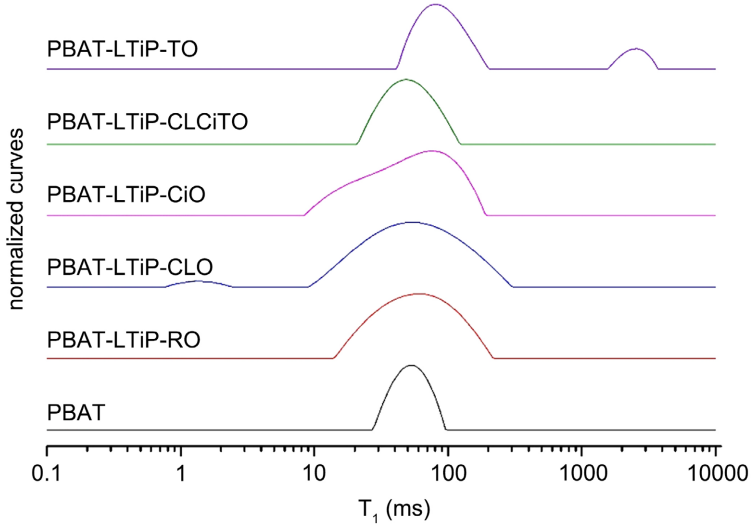

Figure 3. T_1 domain curves of PBAT and composites.

Table 3. T_1 data of PBAT and composites.

Sample	Domain	Estimated start (ms)	Estimated end (ms)	T_1 (ms)
PBAT	1	25	100	52.3
PBAT-LTiP-RO	1	13	210	56.7
PBAT-LTiP-CLO	1	0.5	2.3	1.5
PBAT-LTiP-CLO	2	9	360	54.4
PBAT-LTiP-CiO	1	8	170	16.5; 72.0
PBAT-LTiP-CLCiTO	1	19	130	48.7
PBAT-LTiP-TO	1	27	190	96.9
PBAT-LTiP-TO	2	1500	3500	2500

Table 4 displays the T_2 analysis. The T_2 results show that the incorporation of essential oils significantly altered the distribution between the rigid and mobile domains of PBAT. Neat PBAT exhibited an approximately balanced distribution, with a rigid fraction of 50.93% and a mobile fraction of 49.07%, as well as T_2 values of 25.7 μs for the rigid domain and 426.6 μs for the mobile domain. These values serve as a reference for evaluating the changes induced by the different oils. For the PBAT-LTiP-RO composite, the rigid fraction decreased from 50.93% to 45.90%, while the mobile fraction increased to 54.02%. The T_2 relaxation time also increased from 426.6 to 762.7 μs, suggesting changes in the molecular environments detected by TD-NMR and a greater contribution from protons with slower transverse relaxation. This finding may indicate greater freedom of movement for some of the protons in the sample. However, the slight increase in T_1, from 52.3 to 56.7 ms, cannot be directly associated with either increased or restricted molecular mobility when considered alone, as this parameter is also affected by local molecular environments and proton-proton interactions. It is also important to consider that protons from the rosemary essential oil constituents may contribute to the domains obtained from the TD-NMR data fitting. Thus, the observed changes cannot be attributed solely to the dynamics of the polymer matrix. PBAT-LTiP-CLO composite exhibited an opposite behavior. The rigid fraction increased to 56.25%, while the mobile fraction decreased to 43.75%. Furthermore, T_{2R} increased considerably, from 25.7 to 57.8 μs, whereas T_{2M} decreased from 426.6 to 283.8 μs. This set of results indicates a greater relative contribution from environments with restricted mobility. Although the T_1 value of 54.4 ms remained close to that of pure PBAT (52.3 ms), it must be taken into consideration that the enlargement and displacement of the domain interval to higher relaxation times is an indication that new polymer-filler and polymer-oil interactions had a role in the molecular relaxation distribution. PBAT-LTiP-CiO was even more heteroge-

neous. The rigid fraction decreased to 37.04%, while the mobile fraction increased to 62.96%. T_{2M} also increased to 501.3 μs, exceeding the value observed for PBAT. At the same time, T_1 analysis revealed two values—16.5 and 72.0 ms—indicating the presence of different proton populations or environments. The combination of these two results suggests that the cinnamon oil promoted greater heterogeneity in the material's molecular dynamics. For PBAT-LTiP-TO, the rigid fraction was 53.12% - slightly higher than that of PBAT, while the mobile fraction remained close to the reference value at 46.88%. However, T_{2M} increased to 621.8 μs but T_{2R} decreased to 18.7 μs. The most striking result appears in T_1, which rose from 52.3 ms to 96.9 ms. Thyme oil showed a response distinct from the other oils. While T_1 shifted toward higher relaxation times - indicating reduced molecular mobility - the T_{2R} of the rigid phase decreased - addressing to lower molecular mobility. These results were complementary, leading to the conclusion that the rigid phase governs the molecular relaxation of this composite. For PBAT-LTiP-CLCiTO, the rigid fraction dropped to just 29.07%, while the mobile fraction reached 70.93%. For both fraction, T_2 increased to 31.9 and 1367.2 μs, respectively, for rigid and mobile fraction. This result highlights a significant change in the distribution of PBAT molecular environments meaning increase of molecular mobility in accordance to found for T_1. Summarizing, the results indicate that the LTiP and essential oils induced distinct changes in the molecular dynamics and the distribution of proton environments in PBAT. Rosemary oil and especially the mixing of clove, cinnamon, and thyme increased the contribution of the mobile fraction, whereas clove oil increased the rigid fraction. Cinnamon also increased the mobile fraction but exhibited two T_1 domains, indicating greater heterogeneity. Thyme, in turn, showed the highest T_1 value, although the distribution between the rigid and mobile fractions remained close to that of pure PBAT. Then, TD-NMR has proven to be a suitable technique for studying molecular mobility which can be simultaneously influenced by crystallinity, temperature, composition, and interactions between the polymers and ingredients added to it. The result is in consonance to DRX analysis.

Table 4. T_2 of PBAT and composites.

Samples	T_{2R} (μs)	Rigid fraction (%)	T_{2M} (μs)	Mobile fraction (%)
PBAT	25.7	50.9	426.6	49.1
PBAT-LTiP-RO	20.9	45.9	762.7	54.0
PBAT-LTiP-CLO	57.8	56.3	283.8	43.8
PBAT-LTiP-CiO	27.2	37.0	501.3	62.9
PBAT-LTiP-CLCiTO	31.9	29.1	1367.2	70.9
PBAT-LTiP-TO	18.7	53.1	621.8	46.9

3.4. Thermogravimetry

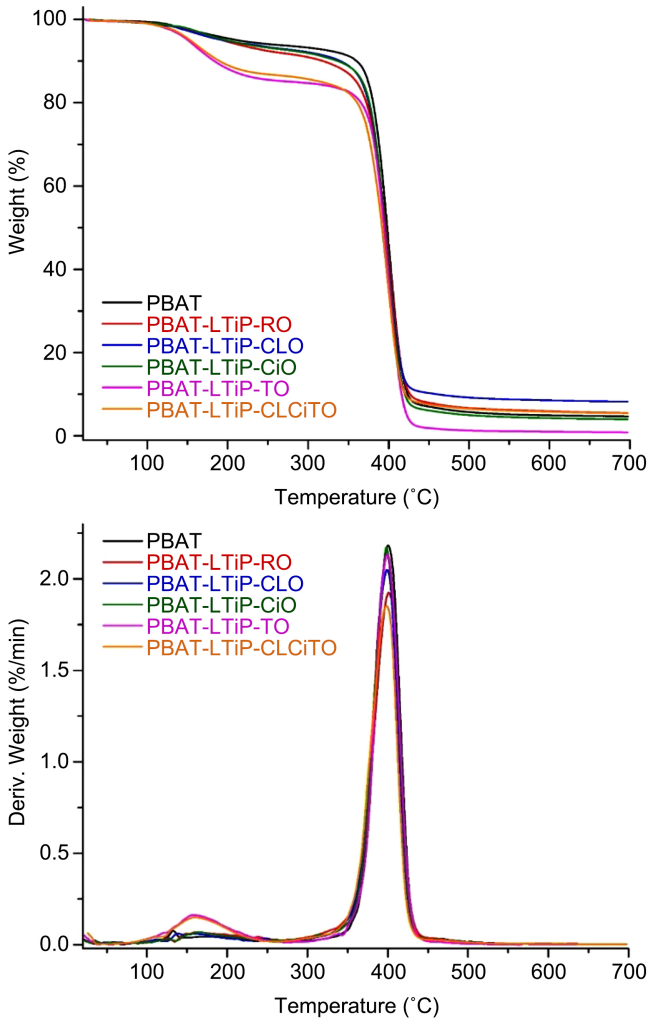

Figure 4. Mass loss and derivative curves of PBAT and composites.

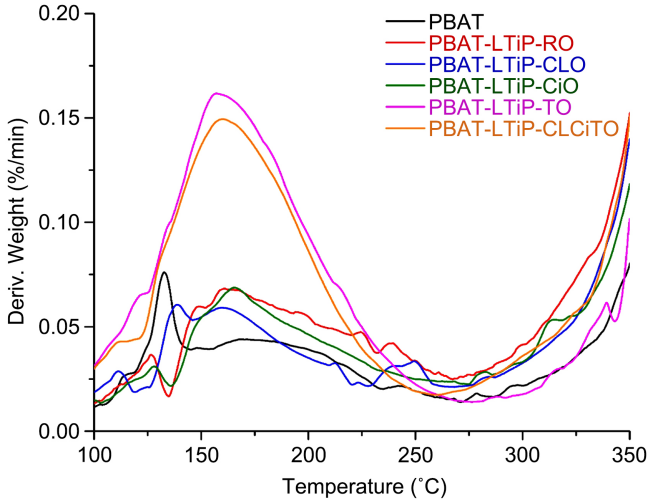

Figure 5. Amplification of TGA derivative curves in the range of 100˚C - 350˚C.

Table 5. Thermogravimetric data of PBAT and composites.

Samples	$T_{5\%}$ (˚C)	$T_{10\%}$ (˚C)	$T_{50\%}$ (˚C)	T_{max} (˚C)	Residue (%) 700˚C
PBAT	211.8	360.2	398.2	400.1	4.7
PBAT-LTiP-RO	193.1	318.0	396.4	401.1	5.5
PBAT-LTiP-CLO	194.2	339.8	395.7	399.1	8.2
PBAT-LTiP-CiO	197.9	336.3	395.6	398.0	4.0
PBAT-LTiP-TO	153.3	189.9	391.7	398.5	5.5
PBAT-LTiP-CLCiTO	150.6	183.3	394.3	399.3	0.8

T_{max} is the temperature where the speed of degradation is maximum; **$T_{5\%}$**, **$T_{10\%}$**, and **$T_{50\%}$** correspond to the temperature where the mass loss were 5%, 10% and 50% while T_m is the temperature where the speed of degradation is maximum.

Figure 4 presents the mass loss and derivative curves. Table 5 compiles the thermogravimetric data. The mass loss curves are separated in two groups. One of them contains the curves of PBAT, PBAT-LTiP-RO, PBAT-LTiP-CLO and PBAT-LTiP-CiO while the other one includes PBAT-LTiP-TO and PBAT-LTiP-CLCiTO. All of them exhibited the following degradation profile: a degradation step around 100˚C - 250˚C, followed by a plateau and a final degradation step in the 350˚C - 450 °C range. PBAT exhibited a $T_{5\%}$ of 211.8˚C, $T_{10\%}$ of 360.2˚C, $T_{50\%}$ of 398.2˚C, and a maximum degradation temperature (T_{max}) of 400.1˚C, with a residue of 4.7% at 700˚C. These values characterize the main thermal degradation stage of the PBAT matrix and can serve as a reference for evaluating the effect of incorporating LTiP and essential oils. For the modified materials, a more pronounced reduction in $T_{5\%}$ and $T_{10\%}$ was observed, particularly in formulations containing thyme oil and the oil blend. PBAT-LTiP-RO showed a $T_{5\%}$ of 193.1˚C and $T_{10\%}$ of 318.0˚C, while PBAT-LTiP-CLO showed 194.2˚C and 339.8˚C, respectively. For PBAT-LTiP-CiO, the values were 197.9˚C and 336.3˚C. Despite these reductions compared to PBAT, the maximum degradation temperatures remained close to those of the polymer, with a T_{max} of 401.1˚C for PBAT-LTiP-RO, 399.1˚C for PBAT-LTiP-CLO, and 398.0˚C for PBAT-LTiP-CiO. This behavior indicates that the incorporation of essential oils primarily affected the initial stages of mass loss without significantly altering the temperature corresponding to the predominant degradation of the PBAT chain. This distinction is important because $T_{5\%}$ and $T_{10\%}$ are particularly sensitive to the presence of components with lower thermal stability, whereas T_{max} is more directly related to the degradation of the polymer chain. Among the formulations evaluated, thyme oil caused the greatest reduction in initial degradation temperatures. PBAT-LTiP-TO exhibited a $T_{5\%}$ of 153.3˚C and a $T_{10\%}$ of 189.9˚C—values considerably lower than the 211.8˚C and 360.2˚C observed for PBAT. However, the T_{max} was 398.5˚C, very close to that observed for PBAT. This result suggests that mass loss at lower temperatures is

primarily associated with the presence of essential oil components characterized by higher volatility or lower thermal stability, while degradation of the polymer matrix occurs subsequently. This behavior is consistent with the results presented by Luna *et al.* [1] for PBAT containing thyme essential oil. The authors observed mass losses at lower temperatures associated with the oil's volatile components, whereas the main PBAT degradation occurred in the approximately 370˚C - 430˚C range. Therefore, the reduction in $T_{5\%}$ and $T_{10\%}$ observed in the present study should not necessarily be interpreted as an equivalent reduction in the thermal stability of the PBAT backbone. This behavior is also similar to that described by Nascimento *et al.* [46] for PBAT films containing rosemary essential oil. The authors observed that incorporating the oil did not cause significant changes to the polymer's main thermal degradation stage. Thus, the results obtained in this study reinforce the possibility that the initial mass losses observed in the oil-containing formulations are primarily related to the oil components rather than the premature decomposition of the PBAT backbone. The result obtained for PBAT-LTiP-TO can also be compared with the work of Albitres *et al.* [47], who evaluated PBAT nanocomposites containing nanocellulose. The authors observed changes in thermal stability following the incorporation of the second phase and attributed part of this behavior to the interaction between the matrix and the incorporated phase. Although the nanocellulose used in that study differs from the LTiP employed here, the results demonstrate that introducing a second phase can alter the initial degradation stages without necessarily causing a significant shift in the main PBAT degradation stage. The formulation containing the oil blend, PBAT-LTiP-CLCiTO, exhibited behavior similar to PBAT-LTiP-TO during the initial degradation stages. Values of 150.6˚C for $T_{5\%}$ and 183.3˚C for $T_{10\%}$ were obtained—the lowest values among all the samples analyzed. However, the T_{max} was 399.3˚C, again close to 400˚C. As with the material containing only thyme oil, the results indicate significant mass loss at relatively low temperatures, followed by the main PBAT degradation stage. The proximity between the $T_{10\%}$ values obtained in this study and those reported by Freitas *et al.* [43] is particularly interesting. The authors studied PBAT composites containing zirconium phosphate and cinnamon oil and observed—for the formulation with the highest oil concentration—an additional event at approximately 190˚C - 200˚C, with a $T_{10\%}$ of 193˚C. In the present study, PBAT-LTiP-TO showed a $T_{10\%}$ of 189.9˚C, and PBAT-LTiP-CLCiTO showed 183.3˚C. Although the formulations are not identical, the similar values suggest that the low-temperature region is related to the presence of components more susceptible to volatilization or decomposition. Freitas *et al.* [43] also observed that the main degradation stage of the materials remained close to 390˚C - 400˚C, even in formulations containing cinnamon oil. This behavior is quite similar to that observed in the present study, where all samples exhibited a T_{max} between 398.0˚C and 401.1˚C. Thus, both the results of Freitas *et al.* [43] and those obtained in the present study indicate that essential oils primarily affect the initial stages of degradation, whereas the predominant decomposition of PBAT occurs at elevated

temperatures. Araújo *et al.* [42] also observed similar behavior in PBAT composites containing zirconium phosphate and clove essential oil. The authors identified an additional mass loss stage at lower temperatures, associated with the presence of essential oil components, while the main degradation stage remained linked to the PBAT. Furthermore, the authors found that the presence of the phosphate could contribute to a slight improvement in thermal stability, depending on the modification applied to the material. In the present study, however, the presence of LTiP did not result in a uniform increase in initial degradation temperatures. This result suggests that the effect of the inorganic phase cannot be analyzed in isolation, as the presence of essential oils also significantly influences thermal behavior. The nature of the phosphate, its dispersion within the matrix, interactions with the PBAT, and the oil composition may all contribute simultaneously to the observed behavior. A comparison of the different formulations reinforces this interpretation. PBAT-LTiP-RO exhibited a $T_{5\%}$ of 193.1˚C, whereas PBAT-LTiP-CLO and PBAT-LTiP-CiO showed values of 194.2˚C and 197.9˚C, respectively. These values are relatively close to one another but lower than those of PBAT. This behavior suggests that the rosemary, clove, and cinnamon oils introduced components that begin to volatilize or decompose prior to the matrix's main degradation stage. Among these materials, PBAT-LTiP-CiO exhibited a $T_{5\%}$ of 197.9˚C, the highest value among the composites containing a single oil. This result indicates that, among the individual formulations, cinnamon oil had the least influence on the initial mass loss stage. Nevertheless, the $T_{10\%}$ value of 336.3˚C remained lower than that observed for PBAT. In a study on PBAT with cinnamon oil and zirconium phosphate, Freitas *et al.* [43] also observed that the presence of the oil altered initial degradation temperatures, particularly as the oil concentration increased. PBAT-LTiP-CLO exhibited a $T_{5\%}$ of 194.2˚C and a $T_{10\%}$ of 339.8˚C, whereas PBAT-LTiP-RO exhibited a $T_{5\%}$ of 193.1˚C and a $T_{10\%}$ of 318.0˚C. Thus, although both materials show similar initial temperatures, the formulation containing rosemary oil displayed a more pronounced reduction in $T_{10\%}$. This result indicates that the effects of the different oils are not equivalent and are likely related to the specific chemical composition of each. Literature also indicates that the presence of a second phase can alter the thermogravimetric behavior of PBAT in a composition-dependent manner. Albitres *et al.* [47] observed that the incorporation of nanocellulose caused changes in the thermal stability of the nanocomposites, a behavior linked to the presence of functional groups capable of influencing degradation processes. In the present study, LTiP and the essential oil components may act similarly in modifying the chemical environment of the matrix, although the underlying mechanisms differ. Another important parameter is $T_{50\%}$. Despite the differences observed in $T_{5\%}$ and $T_{10\%}$, $T_{50\%}$ values remained similar across all formulations: 396.4˚C for PBAT-LTiP-RO, 395.7˚C for PBAT-LTiP-CLO, 395.6˚C for PBAT-LTiP-CiO, 391.7˚C for PBAT-LTiP-TO, and 394.3˚C for PBAT-LTiP-CLCiTO. Compared to PBAT, which exhibited a $T_{50\%}$ of 398.2˚C, the reductions were relatively small. The fact that $T_{50\%}$ remained within

a narrow range, combined with the similarity in T_{max} values, reinforces that the main degradation stage of PBAT was not significantly altered by the incorporation of the oils. The largest difference occurred with PBAT-LTiP-TO, which showed a $T_{50\%}$ of 391.7˚C. Even in this case, the difference relative to PBAT was much smaller than that observed for $T_{5\%}$ and $T_{10\%}$. The residue obtained at 700˚C exhibited more variable behavior. PBAT left a residue of 4.7%, whereas PBAT-LTiP-RO, PBAT-LTiP-CLO, and PBAT-LTiP-TO showed 5.5%, 8.2%, and 5.5%, respectively. The highest value was observed for PBAT-LTiP-CLO. The presence of LTiP—being an inorganic phase—may contribute to increased residue after degradation. However, other factors, such as the dispersion of the inorganic phase and the composition of the products formed during degradation, must also be considered. The result obtained for PBAT-LTiP-CLO is somewhat similar to the behavior described by Araújo *et al.* [42], who observed an increase in residue in composites containing zirconium phosphate. In that study, the increased residue was attributed to the presence of the inorganic phase, which remains after the decomposition of the material's organic fraction. Conversely, PBAT-LTiP-CLCiTO showed only 0.8% residue, a value lower than that of neat PBAT. This result demonstrates that the amount of residue cannot be directly linked solely to the nominal presence of LTiP. The mixture of oils may favor the formation of more volatile products during degradation or alter the distribution of the inorganic phase within the matrix. Therefore, the residue behavior should be interpreted with caution. Freitas *et al.* [43] also observed differences in the residue of composites containing zirconium phosphate and cinnamon oil. In that study, neat PBAT showed a residue of 1.2%, whereas the incorporation of ZrP increased this value to 2.7%, reaching 3.5% in one of the formulations containing modified ZrP and oil. This behavior confirms the potential contribution of the inorganic phase to the final residue but also demonstrates that the presence of the oil can modify this result. Overall, the TGA/DTG results obtained in this work show behavior similar to that described in the literature for PBAT composites containing inorganic phases and essential oils. The main difference among the formulations lies in the temperatures of the initial mass losses, while the predominant degradation stage remains concentrated near 400˚C. Comparison with Freitas *et al.* [43] shows that the $T_{10\%}$ values near 190˚C observed for PBAT-LTiP-TO and PBAT-LTiP-CLCiTO fall within the same range as the additional event identified in PBAT/ZrP/cinnamon oil composites. Meanwhile, results from Araújo *et al.* [42] show that clove oil can also produce mass loss events at lower temperatures without significantly altering the matrix's main degradation. Albitres *et al.* [47], in turn, demonstrated that the incorporation of a second phase can also modify the initial stages of PBAT degradation. Thus, the results suggest that the observed reduction in $T_{5\%}$ and $T_{10\%}$ for the modified materials is primarily related to the presence of essential oil components and their interactions with the matrix and LTiP. The primary degradation stage of PBAT, represented by Tmax and $T_{50\%}$, remained relatively preserved. Among the formulations evaluated, thyme oil and the oil mixing caused the most

significant changes in initial degradation temperatures, whereas cinnamon oil exhibited behavior closest to that of PBAT among the single-oil formulations. Therefore, although the incorporation of essential oils reduced thermal stability during the initial mass loss stages, the materials still maintained their main degradation stage at temperatures near 400˚C. Variation in the residue was ascribed mainly to the oil composition. To better understanding the changes occurred in the range of 100˚C - 350˚C, the amplification was done (**Figure 5**). As can be seen, variations in PBAT could be associated with the addition of compounds in order to improve its processability. In the composites, the observed variations were attributed to the specific compositions of each oil. Mass losses below 50% are related to the compositions of the individual oils. Beyond this threshold, it was observed that the oils and LTiP have, in fact, little influence on the thermal stability of PBAT.

3.5. Differential Scanning Calorimetry

Figure 6 shows the cooling (left one) and second heating (right one) curves. Either the cooling curves or the second heating curves exhibited very similar profiles. Some shifts along the temperature axis were observed. **Table 6** displays the calorimetric data. Regarding the crystallization temperature (T_c), it can be observed that LTiP acted as a nucleating agent for PBAT-LTiP-RO, PBAT-LTiP-CLO and PBAT-LTiP-CiO composites. In the LTiP, the tetravalent titanium ions preferentially maintain an octahedral coordination, similar to that of crystalline materials, but the titanium octahedra and phosphate tetrahedra are connected in an irregular and disordered manner [48]. In those composites, LTiP served as a substrate, facilitating the crystalline organization of the PBAT chains even with its irregular structural arrangement. Conversely, for the PBAT-LTiP-TO and PBAT-LTiP-CLCiTO composites, a retarding effect was noted, indicating that the plasticizing effect of the oils outweighed the nucleating effect of the LTiP. With respect to T_m, crystals with higher melting temperatures were obtained for the PBAT-LTiP-RO and PBAT-LTiP-CLO composites, indicating a greater crystalline perfection. This observation could be attributed to the LTiP nucleating effect. Although an effect on the crystallization temperature (T_c) has been noticed for PBAT-LTiP-CiO, it was not sufficient to result in further improvement in the PBAT crystals. In the case of PBAT-LTiP-TO composite, the oil plasticizing effect was a decisive factor in the reduction of the T_m, while for the PBAT-LTiP-CLCiTO composite, neither LTiP nor oil mixing showed a clear dominance of one over the other. Regarding crystallinity degree (X_c), it is well recognized that PBAT has difficulty crystallizing. Zhou *et al.* [39] reported that the fraction of terephthalic acid in the PBAT composition regulated the rate of crystallization. In their study, it was monitored the action self-assembly nucleating agent octamethylenedicarboxylic dibenzoylhydrazide (OMBH) on the PBAT crystallization. The highest nucleation efficiency was around 60% by adding 0.7 wt% OMBH [39]. Li *et al.* [49] investigated two types of PBAT, PBAT-A and PBAT-C, with the same fraction of 1,4-butanediol (BDO).

PBAT-A constitution contains adipic acid (AA, 0.52), and terephthalic acid (TA, 0.480) while PBAT-C comprises AA (0.525) and TA (0.475). Calorimetric data indicated that both revealed a low degree of crystallization around 7% and 8%, for PBAT-A and PBAT-C, respectively. Freitas *et al.* [43] studied composites of PBAT embedded with zirconium phosphate, as prepared and intercalated with amine, and cinnamon oil. The author reported an increase in the degree of crystallinity from around 9% - 70% besides the displacement of crystallization temperature to higher values. Similar results were found by Araújo *et al.* [42] in their study on PBAT enriched with zirconium phosphate and clove oil. Herein, all composites revealed that X_c values remained below those observed for single PBAT. Although some nucleation effect has been noticed, the action of the oils was to disperse the crystallization centers, which indicates that they play an important role in the crystallization of PBAT. While LTiP may have contributed to the PBAT crystallization process, this contribution was not sufficient to outweigh the effect of the oils in dispersing the crystallization centers. It should be taken into account that polymer-oil interactions could have also contributed to the calorimetric results. The analyses FTIR, DRX, TDNMR, and TGA corroborated the calorimetric data.

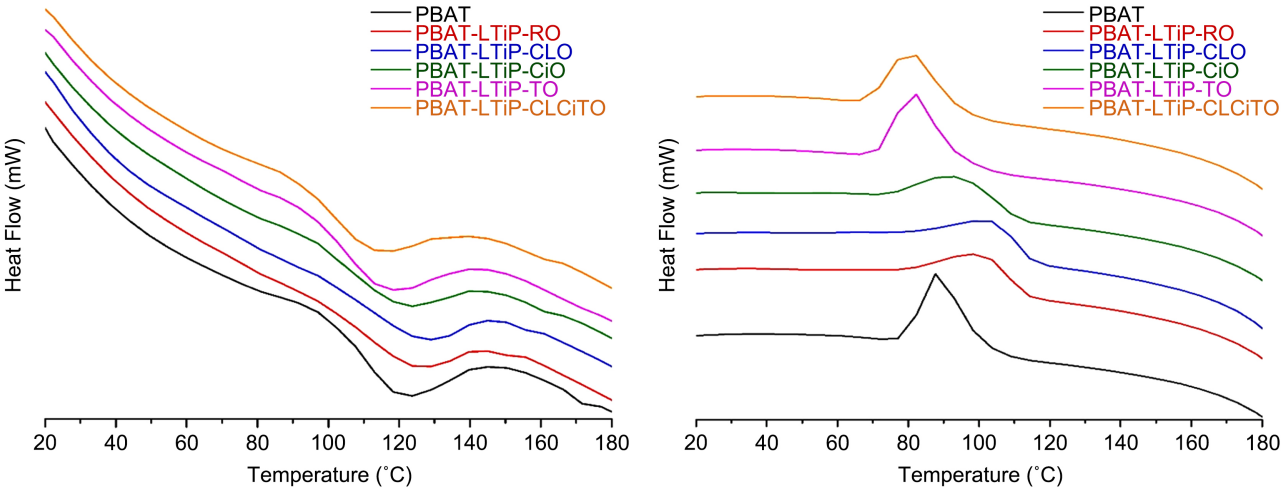

Figure 6. Cooling (left one) and second heating (right one) curves.

Table 6. Calorimetric data of PBAT and composites.

Samples	T_c (˚C)	Crystallization temperature interval (˚C)	T_m (˚C)	Melting temperature interval (˚C)	ΔH_m (J/g)	X_c%
PBAT	88	93 - 82 ΔT = 11	118	102 - 140 ΔT = 38	11.49	15
PBAT-LTiP-RO	98	104 - 82 ΔT = 22	124	102 - 140 ΔT = 38	7.43	9.9
PBAT-LTiP-CLO	98	104 - 82 ΔT = 22	124	102 - 140 ΔT = 38	7.86	11
PBAT-LTiP-CiO	93	98 - 77 ΔT = 21	118	102 - 140 ΔT = 38	7.72	10
PBAT-LTiP-TO	82	88 - 72 ΔT = 16	113	102 - 134 ΔT = 32	6.76	9
PBAT-LTiP-CLCiTO	82	88 - 77 ΔT = 11	118	102 - 140 ΔT = 38	9.38	13

3.6. Scanning Electron Microscopy (SEM)

Figure 7 shows the images of the scanning electron microscopy (SEM) before and after etching on the longitudinal surface of the composite films, during seven days. Table 7 displays the mass loss of each composite. The oil release of each composite obeyed the following sequence: PBAT-LTiP-RO < PBAT-LTiP-CLO < PBAT-LTiP-CiO < PBAT-LTiP-CLCiTO < PBAT-LTiP-TO. The result evidenced that the oil release is associated with the designed interaction among polymer-oil, polymer-filler and filler-oil. Another important aspect is the behavior observed for the film containing the blend of essential oils. The mass loss of 11.90% was higher than that observed individually for the films containing clove and cinnamon, and close to the value obtained for the film with thyme oil. This result may indicate that there must be simultaneous presence of various molecules with different chemical natures and polarities, which are capable of forming distinct interactions with the PBAT matrix and the LTiP. Another piece of evidence associated with the oil composition is clearly shown when etching results of PBAT-LTiP-RO and PBAT-LTiP-TO composites are compared. Rosemary oil (main component is eucalyptol) and thyme oil (main component is thymol) exhibited mass loss of 5.10 wt.% and 13.51 wt.%, respectively. This indicates that the mere presence of an essential oil does not, by itself, determine the behavior of the film during etching. The chemical composition of the oil, its affinity for the polymer matrix, its distribution within the film, and its interaction with the LTiP likely all contribute to this behavior. The literature confirms that the incorporation of essential oils can significantly modify the structure and properties of PBAT films. Moraes Filho *et al.*, for instance, produced PBAT films containing 2, 4 and 8 wt.% of clove and cinnamon essential oils using the solution casting method. The authors observed that the oils were able to migrate from the polymer matrix into the surrounding medium, demonstrating that the interaction between the oil and the PBAT matrix does not entirely prevent the mobility of these molecules [50]. Therefore, the mass loss values obtained in this analysis demonstrate that the etching treatment was capable of inducing measurable changes in the films, and that these changes depend on the formulation composition and obviously the interactions among polymer, essential oil and filler.

Table 7. Mass loss after etching process.

Composite	Mass (before etching) (g)	Mass (after etching) (g)	Mass loss (%)
PBAT-LTiP-RO	0.0236	0.0224	5.10
PBAT-LTiP-CLO	0.0167	0.0152	8.98
PBAT-LTiP-CiO	0.0133	0.0121	9.02
PBAT-LTiP-TO	0.0148	0.0128	13.51
PBAT-LTiP-CLCiTO	0.0353	0.0311	11.90

PBAT-LTiP-RO

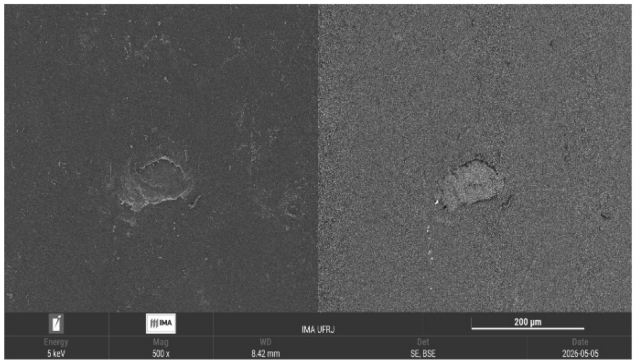

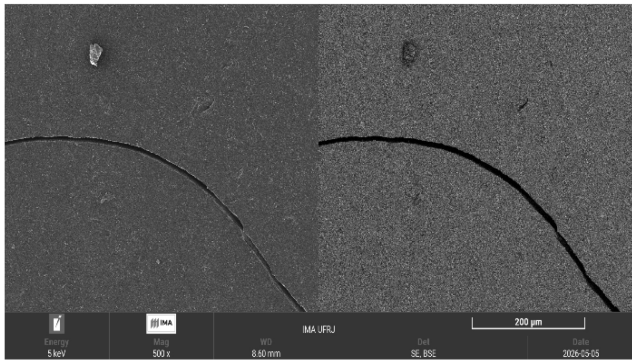

PBAT-LTiP-CLO

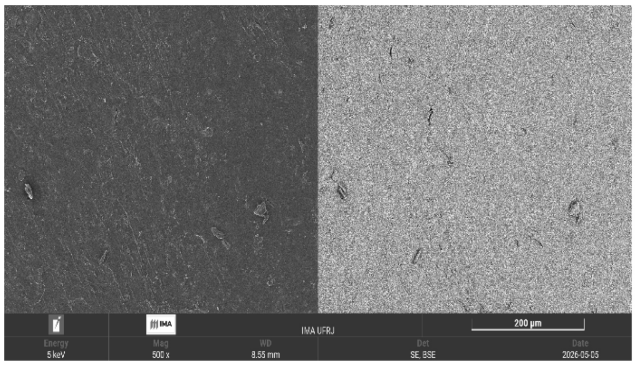

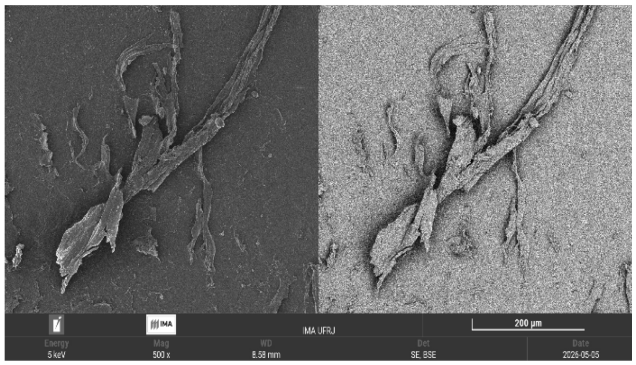

PBAT-LTiP-CiO

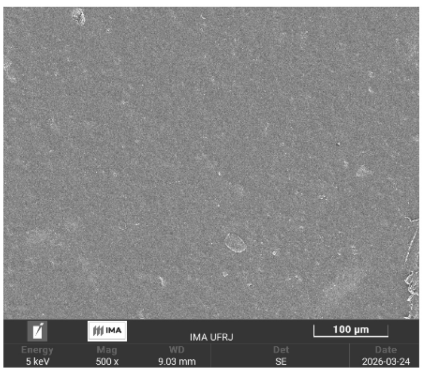

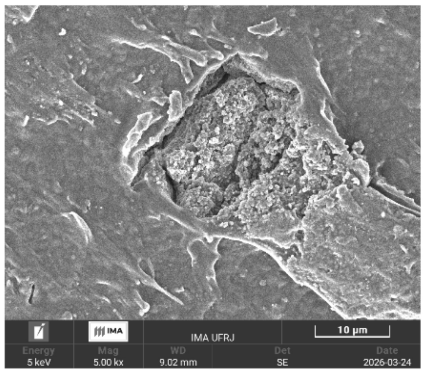

PBAT-LTiP-TO

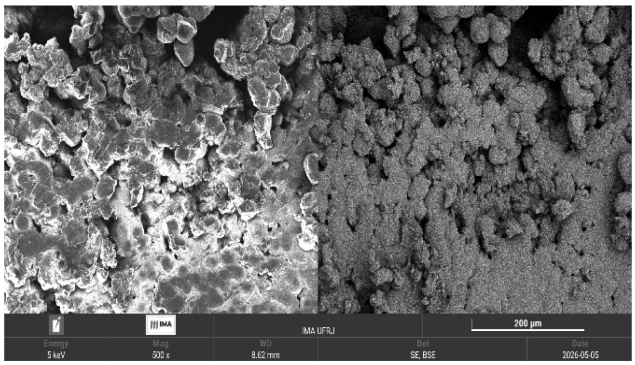

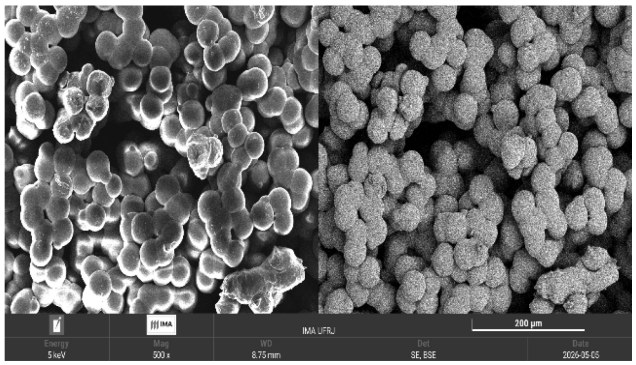

PBAT-LTiP-CLCiTO

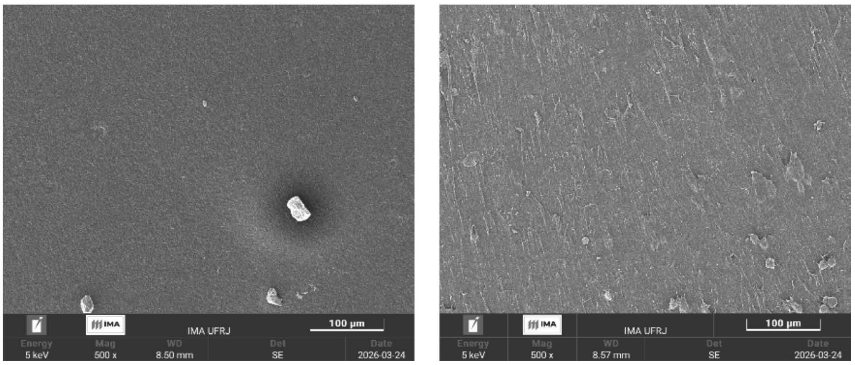

Figure 7. SEM images of composites 500 X before (left) and after etching (right).

3.7. Antimicrobial Evaluation

Table 8 exhibits the antimicrobial activity of the composites against bacteria and yeast by using the agar diffusion method. Singly PBAT did not produce inhibition zones against the bacteria tested, indicating that the polymer, under the conditions employed, exhibited no detectable antimicrobial activity. The incorporation of essential oils, however, altered this behavior, resulting in the formation of inhibition zones, the intensity of which depended on both the specific oil used and the microorganism being tested. For *Escherichia coli*, inhibition zones of 12, 8, 8, and 10 mm were observed for films of the composites PBAT-LTiP-CiO, PBAT-LTiP-TO, PBAT-LTiP-CL and PBAT-LTiP-CLCiTO, respectively. The largest inhibition zone was obtained with the film containing cinnamon oil (12 mm), which is consistent with the well-known antimicrobial activity of this oil, an effect primarily attributed to the presence of cinnamaldehyde, its major bioactive constituent. However, the antimicrobial activity of essential oils does not depend solely on an individual compound, as interactions between various constituents can influence the observed response. Similar results were reported by Freitas *et al.* [43], who developed composite films based on poly(butylene adipate-co-terephthalate) (PBAT), zirconium phosphate, and cinnamon essential oil. The authors prepared formulations containing 2 wt% zirconium phosphate modified with ethylenediamine (ZrP/ED) and different concentrations of cinnamon essential oil (CEO), corresponding to 5 and 10 wt% relative to the PBAT mass. The PBAT/ZrP/ED/CEO10 formulation, containing 10 wt% cinnamon essential oil, exhibited an inhibition zone of 14 mm against *Escherichia coli*. This result is close to that obtained in the present study, in which the film containing cinnamon essential oil exhibited an inhibition zone of 12 mm against the same bacterial strain. The similarity between these values indicates that the antimicrobial activity of cinnamon essential oil can also be maintained after its incorporation into different polymer matrices [43]. For Staphylococcus aureus, inhibition zones of 11 mm were observed for PBAT-LTiP-CiO composite, 7 mm for PBAT-LTiP-TO composite, and 10 mm for PBAT-LTiP-CLCiTO. The larger inhibition zone obtained for PBAT-LTiP-CiO is consistent with studies that attribute the antimicrobial activity of this oil to its

high concentration of cinnamaldehyde. Ooi *et al.* [51] demonstrated significant activity of cinnamon oil and cinnamaldehyde against various bacterial species, including S. aureus. Cinnamaldehyde can act upon the cell membrane and interfere with essential metabolic processes, thereby compromising the viability of microbial cells. The behavior observed for Bacillus cereus was even more pronounced with PBAT-LTiP-CiO composite, which exhibited a 14 mm inhibition zone. For PBAT-LTiP-CLCiTO composite, significant activity, with a 13 mm inhibition zone, was achieved. These results underscore the importance of cinnamon oil in the antimicrobial performance of the films, particularly against Gram-positive bacteria. The observed activity is consistent with previous studies that have demonstrated the efficacy of cinnamon oil and cinnamaldehyde against various bacteria, including species of the genus Bacillus [51]. Regarding Enterococcus faecalis, only PBAT-LTiP-CLCiTO composite exhibited activity, producing an 8 mm inhibition zone. Similarly, Lactobacillus acidophilus showed an inhibition zone exclusively in the presence of that composite, with a measurement of 9 mm. This behavior is particularly noteworthy because none of the oils, when evaluated individually, produced a measurable inhibition zone against these two species under the conditions tested. Thus, the combination of the oils resulted in an expanded antimicrobial spectrum, making this material a promising candidate - compared to the other samples -for the inhibition of bacteria and fungi. The greatest antimicrobial activity observed in the study was, however, against the yeast Candida albicans. The inhibition zones measured 8 mm for PBAT, 15 mm for PBAT-LTiP-CLO, 32 mm for PBAT-LTiP-CiO, 13 mm for PBAT-LTiP-TO, and 24 mm for PBAT-LTiP-CLCiTO. It is important to note that, since no analyses were performed on PBAT/LTiP films without essential oils or on samples containing only the solvent, the individual contributions of titanium phosphate and potential residual solvent to the observed results could not be independently determined. Notably, PBAT-LTiP-CiO exhibited a 32 mm inhibition zone—a value considerably higher than those observed for the bacteria. This result is particularly consistent with the study by Freitas *et al.* [43], who developed PBAT composites containing zirconium phosphate and cinnamon essential oil and also observed an inhibition zone of approximately 32 mm against *C. albicans*. This similarity in results is significant because it was obtained using polymeric systems based on the same polymer and containing cinnamon oil, even though different types of phosphate were employed. The high antifungal activity of cinnamon oil also aligns with findings reported by Ooi *et al.* [51], who demonstrated the activity of *Cinnamomum cassia* oil and cinnamaldehyde against various Candida species, including *C. albicans*. Cinnamaldehyde is considered a primary contributor to this activity, as it can compromise the integrity of the fungal cell and interfere with metabolic processes essential for its survival. Thus, the agreement between the results obtained in this work and those reported by Freitas *et al.* [43] reinforces the contribution of cinnamon oil to the antifungal activity of PBAT composites, regardless of the type of phosphate incorporated into the matrix. PBAT-LTiP-CLO composite exhibited

significant activity against *C. albicans*, with a 15 mm inhibition zone. This behavior may be attributed to the presence of eugenol, one of the primary constituents of clove oil and a compound widely studied for its antimicrobial activity. Eugenol can alter cell membrane permeability and cause the loss of intracellular components, in addition to interfering with metabolic processes. Marchesi [9] highlighted that the antimicrobial activity of eugenol is primarily associated with its interaction with the cell membrane and the disruption of its integrity. PBAT-LTiP-CLCiTO also exhibited high antifungal activity, with a 24 mm inhibition zone. Although this value was lower than that obtained for cinnamon oil alone, the mixture showed activity against all the microorganisms evaluated. This behavior indicates that combining the oils does not necessarily increase the intensity of activity against every microorganism, but it may contribute to broadening the spectrum of antimicrobial action. The results should also be interpreted by considering the incorporation of the oils into the PBAT/LTiP matrix. The formation of inhibition zones depends not only on the antimicrobial activity of the oils but also on their ability to migrate from the polymer matrix and diffuse into the culture medium. Studies on PBAT films containing essential oils demonstrate that the release of active compounds from the matrix is directly related to the material's antimicrobial performance. Moraes Filho *et al.* [50], for instance, observed antimicrobial activity in PBAT films containing clove and cinnamon oils, attributing this effect to the presence and release of the bioactive compounds incorporated into the polymer. Similarly, Tian *et al.* [11] showed that PBAT films containing cinnamon essential oil exhibited activity against E. coli and S. aureus, highlighting the influence of the oil's release behavior on its antimicrobial activity. In this sense, the differences observed among the films may be related both to the chemical composition of the oils and to the way their constituents interact with the PBAT/LTiP matrix. The structure and polarity of the compounds, their volatility, and their affinity for the polymer matrix can influence the amount effectively released into the culture medium. Thus, an oil with high intrinsic activity may exhibit a relatively small halo if its release or diffusion is limited. Overall, the results show that the incorporation of essential oils imparted antimicrobial activity to the PBAT/LTiP films, with the effect varying depending on the microorganism. Cinnamon made the greatest contribution to antifungal activity, particularly against *C. albicans*, while thyme oil showed higher activity against E. coli. The blend of clove, cinnamon, and thyme exhibited the broadest spectrum of action, being the only treatment capable of producing inhibition zones against *E. faecalis* and L. acidophilus. These findings are relevant to the development of active polymeric materials, as they demonstrate that combining different essential oils can provide PBAT/LTiP with a broader range of antimicrobial activity.

Finally, in **Figure 8** are shown the projected interactions among PBAT, the oils, and LTiP. As can be seen, all the main constituents of the oils are potentially available for interaction with LTiP. Only thymol and eugenol besides LTiP are enabled to interact with PBAT. The interactions of LTiP with PBAT and the oils signifi-

cantly influenced the results obtained from XRD, TD-NMR, and DSC techniques. For TDNMR analysis, with the exception of the PBAT-LTiP-TO composite, which exhibited relaxation domains with distinct time constants, no single interaction predominates over the others; however, a shift toward longer relaxation times is evident, resulting from the PBAT/LTiP interaction. For crystallization temperature (T_c), it can be deduced that the interaction LTiP/PBAT regulated this calorimetric parameter for PBAT-LTiP-RO, PBAT-LTiP-CLO and PBAT-LTiP-CiO composites. Regarding the melting temperature (T_m), LTiP was the dominant factor for PBAT-LTiP-RO and PBAT-LTiP-CLO, while for PBAT-LTiP-TO thymol/PBAT interaction was the dominant factor.

PBAT

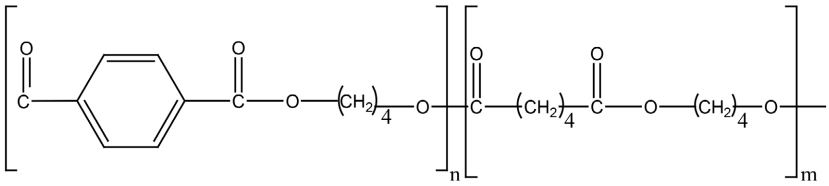

	Interaction with PBAT	Interaction with LTiP
Thymol	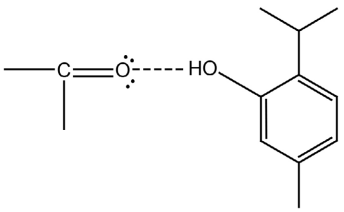	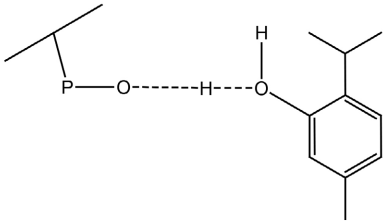
Eucalytol	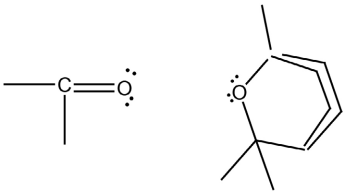	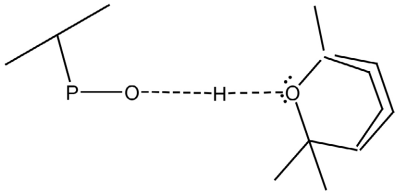
Eugenol	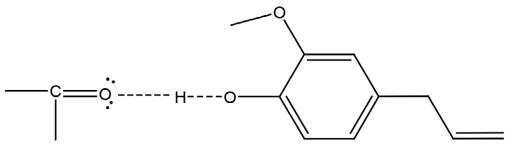	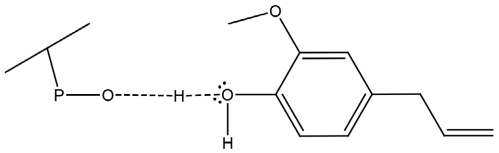
Cinnamaldehyde	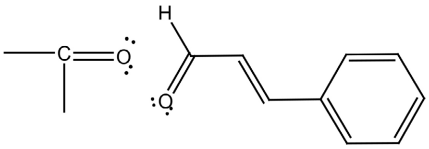	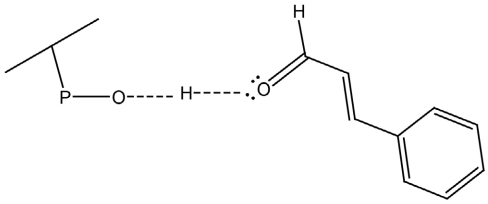
LTiP	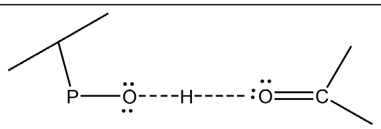	----------

Figure 8. Designed interactions among PBAT, oils and LTiP.

Table 8. Antimicrobial activity of the composites against bacteria and yeast.

Microorganisms (ATCC number)	Zone of inhibition (mm^{-1})					
	PBAT	PBAT-LTiP -RO	PBAT-LTiP -CLO	PBAT-LTiP -CiO	PBAT-LTiP -TO	PBAT-LTiP -CLCiTO
Bacteria						
Escherichia coli ATCC 11229	--	--	8	12	8	10
Staphylococcus aureus ATCC 29213	--	--	--	11	7	10
Bacillus cereus ATCC 14579	--	--	7	14	--	13
Enterococcus faecalis ATCC 19433	--	--	--	--	--	8
Lactobacillus acidophilus NCFM (ATCC SD5221)	--	--	--	--	--	9
Yeast						
Candida albicans ATCC 10231	8	--	15	32	13	24

4. Conclusion

Biodegradable composites have been developed. The incorporation of rosemary, clove cinnamon and thyme essential oils into the films revealed interesting findings regarding physicochemical and antimicrobial activity. For all oils, their composition played an important role mainly in the calorimetric and antimicrobial evaluations. The broader observed antimicrobial spectrum of the mixture of clove, cinnamon, and thyme oils should be highlighted, as it demonstrated significant antimicrobial activity against oral bacteria such as Enterococcus faecalis and Lactobacillus acidophilus.

Conflicts of Interest

The authors declare no conflicts of interest regarding the publication of this paper.

References

[1] Luna, P.B.F.G.S., Caetano, V.F., Andrade, M.F., Silva, I.D.L., Araújo, T.L., Souza, K.C., *et al.* (2024) Effect of Thyme Essential Oil on the Properties of Poly(Butylene Adipate-*co*-Terephthalate) (PBAT). *Polímeros*, **34**, e20240005. https://doi.org/10.1590/0104-1428.20230009

[2] Lv, C., Zhou, X., Liu, S. and Su, T. (2026) Enhancing the Performance of PBAT Composites via Incorporation of Nano TiO_2-Tannic Acid Hybrid Filler. *Journal of Polymers and the Environment*, **34**, Article No. 224. https://doi.org/10.1007/s10924-026-03941-0

[3] Wu, Z., Shen, Z., Xu, L., Tong, F., Shan, C., Li, F., *et al.* (2026) Effects of Potassium Dimethyl 5-Sulfoisophthalate as a Nucleating Agent on RCF/PBAT Composites. *Journal of Thermoplastic Composite Materials*, 1-26. https://doi.org/10.1177/08927057261488776

[4] Dong, Y., Su, S., Yang, H., Han, Z., Huang, D., Han, X., *et al.* (2026) Assessing the

Biodegradation of Lignin/PBAT Composites: A Comparative Study of Weight Loss and Mineralization. *Polymers*, **18**, Article 2010. https://doi.org/10.3390/polym18162010

[5] Sarmin, S.N., Karim, Z., Jawaid, M., Ismail, A.S. and Hamdan, M.H. (2026) Impact of Chitosan Incorporation on PBAT Composite: Thermal, Viscoelastic, Mechanical, and Morphological Properties. *Journal of Applied Polymer Science*, **143**, e7109. https://doi.org/10.1002/app.71096

[6] Xu, H., Ma, X., Zhang, M., Dong, F., Xu, P. and Ding, Y. (2026) Synergistic Enhancement of Compatibility, Flame Retardancy and Mechanical Properties of PLA/PBAT Composites by Sulfonic Acid-Based Ionic Liquid, Ammonium Polyphosphate and Boron Nitride. *European Polymer Journal*, **255**, Article 114928. https://doi.org/10.1016/j.eurpolymj.2026.114928

[7] Keskes, M., Desse, M., Carrot, C. and Jaziri, M. (2026) PBAT Composites with Cellulosic Fillers: From Nanocrystals to Isometric Particles, Effect of Aspect Ratio, Crystallinity and Dual Filler Combination. *International Journal of Lightweight Materials and Manufacture*, In Press. https://doi.org/10.1016/j.ijlmm.2026.05.003

[8] Zhao, C., Yan, X., Zhou, Z., Guo, L., Yang, S., Chen, Z., *et al.* (2026) Homogeneously Blending PBAT with Silanized Cellulose for Composite Film: Characterization and Physicochemical Property. *Polymers*, **18**, Article No. 875. https://doi.org/10.3390/polym18070875

[9] Marchese, A., Barbieri, R., Coppo, E., Orhan, I.E., Daglia, M., Nabavi, S.F., *et al.* (2017) Antimicrobial Activity of Eugenol and Essential Oils Containing Eugenol: A Mechanistic Viewpoint. *Critical Reviews in Microbiology*, **43**, 668-689. https://doi.org/10.1080/1040841x.2017.1295225

[10] Freires, I., Denny, C., Benso, B., De Alencar, S. and Rosalen, P. (2015) Antibacterial Activity of Essential Oils and Their Isolated Constituents against Cariogenic Bacteria: A Systematic Review. *Molecules*, **20**, 7329-7358. https://doi.org/10.3390/molecules20047329

[11] Tian, Y., Lei, Q., Yang, F., Xie, J. and Chen, C. (2024) Development of Cinnamon Essential Oil-Loaded PBAT/Thermoplastic Starch Active Packaging Films with Different Release Behavior and Antimicrobial Activity. *International Journal of Biological Macromolecules*, **263**, Article 130048. https://doi.org/10.1016/j.ijbiomac.2024.130048

[12] Yanakiev, S. (2020) Effects of Cinnamon (Cinnamomum Spp.) in Dentistry: A Review. *Molecules*, **25**, Article 4184. https://doi.org/10.3390/molecules25184184

[13] Zhang, Y., Wang, Y., Zhu, X., Cao, P., Wei, S. and Lu, Y. (2017) Antibacterial and Antibiofilm Activities of Eugenol from Essential Oil of *Syzygium aromaticum* (L.) Merr. & L. M. Perry (Clove) Leaf against Periodontal Pathogen *Porphyromonas gingivalis*. *Microbial Pathogenesis*, **113**, 396-402. https://doi.org/10.1016/j.micpath.2017.10.054

[14] de Oliveira Carvalho, I., Purgato, G.A., Píccolo, M.S., Pizziolo, V.R., Coelho, R.R., Diaz-Muñoz, G., *et al.* (2020) *In Vitro* Anticariogenic and Antibiofilm Activities of Toothpastes Formulated with Essential Oils. *Archives of Oral Biology*, **117**, Article 104834. https://doi.org/10.1016/j.archoralbio.2020.104834

[15] Kannan, K.P. and Smiline Girija, A.S. (2026) Endodontic Potential of Eugenol against *Enterococcus faecalis*: Antibacterial, Antibiofilm, and Network Pharmacology Insights. *Journal of Oral Biology and Craniofacial Research*, **16**, Article 101532. https://doi.org/10.1016/j.jobcr.2026.101532

[16] Dewi, L.M., Atmaja, A.T., Putra, M.M.R.A., Rosyidah, D.U., Nurhayani, N. and

Munawaroh, R. (2026) *In Vitro* Study of the Antibiofilm Potential of Bay Leaf Extract (*Syzygium polyanthum* (Wight) Walp) against *Streptococcus sanguinis* and *Streptococcus mutans*. *Biology, Medicine, & Natural Product Chemistry*, **15**, 1145-1152. https://doi.org/10.14421/biomedich.2026.151.1145-1152

[17] Akbar, T., Hasan, H., Ghose, R., Yeasmeen, W., Zaman, S., Kabir, M., *et al.* (2025) Effectiveness of *Syzygium aromaticum* in Reducing Dental Plaque Forming Bacteria. *Barind Medical College Journal*, **11**, 130-135. https://doi.org/10.70818/bmcj.v011i2.0233

[18] Zainal-Abidin, Z., Juffry, J.I.M., Najib, N.A.M., Sulaiman, W.N., Shafiei, Z. and Said, M.M. (2025) Antibacterial Effect of Halia Bentong Ethanolic Extract on *Porphyromonas gingivalis*: A Preliminary Investigation. *Malaysian Journal of Medicine and Health Sciences*, **21**, 47-55.

[19] Christopoulou, S.D., Androutsopoulou, C., Hahalis, P., Kotsalou, C., Vantarakis, A. and Lamari, F.N. (2021) Rosemary Extract and Essential Oil as Drink Ingredients: An Evaluation of Their Chemical Composition, Genotoxicity, Antimicrobial, Antiviral, and Antioxidant Properties. *Foods*, **10**, Article 3143. https://doi.org/10.3390/foods10123143

[20] Wang, H., Yih, K., Yang, C. and Huang, K. (2017) Anti-Oxidant Activity and Major Chemical Component Analyses of Twenty-Six Commercially Available Essential Oils. *Journal of Food and Drug Analysis*, **25**, 881-889. https://doi.org/10.1016/j.jfda.2017.05.007

[21] Najmi, Z., Scalia, A.C., De Giglio, E., Cometa, S., Cochis, A., Colasanto, A., *et al.* (2023) Screening of Different Essential Oils Based on Their Physicochemical and Microbiological Properties to Preserve Red Fruits and Improve Their Shelf Life. *Foods*, **12**, Article 332. https://doi.org/10.3390/foods12020332

[22] Florina, C.L., Diana, P., Bernadette-Emoke, T., Bianca-Eugenia, S., Stergiopoulos, C., Krokida, M., Maramathas, I., *et al.* (2026) Phytobiotic Essential Oils as Antibiotic Alternatives in Aquaculture: Antimicrobial and Antioxidant Properties of Garlic, Thyme, Thyme Conehead, Rosemary, and Eucalyptus. *Food Science & Nutrition*, **14**, e71739.

[23] Xiao, H., Lu, W. and Yeh, J. (2009) Crystallization Behavior of Fully Biodegradable Poly(Lactic Acid)/Poly(Butylene Adipate - *co* - Terephthalate) Blends. *Journal of Applied Polymer Science*, **112**, 3754-3763. https://doi.org/10.1002/app.29800

[24] Azevedo, J.V.C., Ramakers-van Dorp, E., Grimmig, R., Hausnerova, B. and Möginger, B. (2022) Process-Induced Morphology of Poly(Butylene Adipate Terephthalate)/Poly(Lactic Acid) Blown Extrusion Films Modified with Chain-Extending Cross-Linkers. *Polymers*, **14**, Article 1939. https://doi.org/10.3390/polym14101939

[25] Biernasiuk, A., Baj, T. and Malm, A. (2022) Clove Essential Oil and Its Main Constituent, Eugenol, as Potential Natural Antifungals against Candida Spp. Alone or in Combination with Other Antimycotics Due to Synergistic Interactions. *Molecules*, **28**, Article 215. https://doi.org/10.3390/molecules28010215

[26] Truzzi, E., Durante, C., Bertelli, D., Catellani, B., Pellacani, S. and Benvenuti, S. (2022) Rapid Classification and Recognition Method of the Species and Chemotypes of Essential Oils by ATR-FTIR Spectroscopy Coupled with Chemometrics. *Molecules*, **27**, Article 5618. https://doi.org/10.3390/molecules27175618

[27] Janusz, W., Khalameida, S., Skwarek, E., Skubiszewska-Zięba, J., Sydorchuk, V. and Charmas, B. (2019) Modification of Titanium Phosphate Precipitated from Titanylsulfate. *Journal of Thermal Analysis and Calorimetry*, **135**, 2925-2934. https://doi.org/10.1007/s10973-018-7611-2

[28] Amghouz, Z., Mendoza-Meroño, R. and Adawy, A. (2023) Nucleation & Growth of

α-Ti$(HPO_4)_2 \cdot H_2O$ Single-Crystal and Its Structure Determination from X-Ray Single-Crystal Data. *Journal of Solid State Chemistry*, **327**, Article 124251. https://doi.org/10.1016/j.jssc.2023.124251

[29] Rodrigues, B.V.M., Silva, A.S., Melo, G.F.S., Vasconscellos, L.M.R., Marciano, F.R. and Lobo, A.O. (2016) Influence of Low Contents of Superhydrophilic MWCNT on the Properties and Cell Viability of Electrospun Poly (Butylene Adipate-*co*-Terephthalate) Fibers. *Materials Science and Engineering*: *C*, **59**, 782-791. https://doi.org/10.1016/j.msec.2015.10.075

[30] Nawaz, T., Ullah, N., Ali, M., Rab, S.O., Ahmad, I., Baloch, R., *et al.* (2025) Formulation Development, Characterization, and Optimization of Eudragit-Cinnamon Essential Oil-Based Nanoplatform and Its Efficacy against Resistant Bacteria. *Frontiers in Chemistry*, **13**, Article ID: 1555449. https://doi.org/10.3389/fchem.2025.1555449

[31] EL-Mekkawi, D.M., Othman, S.A., Abd El-Wahab, R.M. and Selim, M.M. (2023) Easily Prepared Titanium Phosphate-Based Composites for the Remediation of Synthetic and Real Wastewaters. *Water, Air, & Soil Pollution*, **234**, Article No. 249. https://doi.org/10.1007/s11270-023-06256-1

[32] Berraaouan, D., Essifi, K., Addi, M., Hano, C., Fauconnier, M. and Tahani, A. (2023) Hybrid Microcapsules for Encapsulation and Controlled Release of Rosemary Essential Oil. *Polymers*, **15**, Article 823. https://doi.org/10.3390/polym15040823

[33] Silva, K.D.E. da, Vitorino, G.B. de L., Nascimento, C.K. da S., Souza, C.A. de, Barros, A.C. de O.D., *et al.* (2025) Fotodegradação no clima semiárido em filmes de poli(butileno adipato-*co*-tereftalato) puros e aditivados com óleo essencial de cravo da Índia (*Syzygium aromaticum* (L.) Merr.). *Química Nova*, **48**, e-20250097. https://doi.org/10.21577/0100-4042.20250097

[34] Pires Costa, E., Maciel dos Santos, M., de Paula, R.A., da Silva, D.A., Lopes, R.P., Teixeira, R.R., *et al.* (2025) Antioxidant and Anti-Inflammatory Activity of Eugenol, Bis-Eugenol, and Clove Essential Oil: An *in Vitro* Study. *ACS Omega*, **10**, 31033-31045. https://doi.org/10.1021/acsomega.5c04146

[35] Bertuola, M., Fagali, N. and Fernández Lorenzo de Mele, M. (2020) Detection of Carvacrol in Essential Oils by Electrochemical Polymerization. *Heliyon*, **6**, e03714. https://doi.org/10.1016/j.heliyon.2020.e03714

[36] Aversa, C. and Barletta, M. (2022) Addition of Thermoplastic Starch (TPS) to Binary Blends of Poly(Lactic Acid) (PLA) with Poly(Butylene Adipate-*co*-Terephthalate) (PBAT): Extrusion Compounding, Cast Extrusion and Thermoforming of Home Compostable Materials. *Chinese Journal of Polymer Science*, **40**, 1269-1286. https://doi.org/10.1007/s10118-022-2734-0

[37] Fukushima, K., Wu, M., Bocchini, S., Rasyida, A. and Yang, M. (2012) PBAT Based Nanocomposites for Medical and Industrial Applications. *Materials Science and Engineering*: *C*, **32**, 1331-1351. https://doi.org/10.1016/j.msec.2012.04.005

[38] Zhang, J., Hu, D., Wei, S., Xi, Z., Zhen, W. and Zhao, L. (2023) Effects of Chain Composition of PBAT on the Supercritical CO_2 Foaming and Degradation Behavior. *Journal of CO_2 Utilization*, **72**, Article 102500. https://doi.org/10.1016/j.jcou.2023.102500

[39] Zhou, C., Chen, K., Zhang, Z., Jing, M., Liu, C., Shen, C., *et al.* (2024) Enhanced Crystallization of Poly(Butylene Adipate-*co*-Terephthalate) by a Self-Assembly Nucleating Agent. *Chinese Journal of Polymer Science*, **42**, 663-674. https://doi.org/10.1007/s10118-024-3092-x

[40] Li, Y., Feng, T., Liu, J., Pan, C., Wang, Y., Wu, Z., *et al.* (2025) Preparation and Properties of Nano-Lignin-Reinforced Poly(Butylene Adipate-Co-Terephthalate) Com-

posites. *Processes*, **13**, Article 3507. https://doi.org/10.3390/pr13113507

[41] Schmutz, C., Barboux, P., Ribot, F., Taulelle, F., Verdaguer, M. and Fernandez-Lorenzo, C. (1994) EXAFS, Raman and 31P NMR Study of Amorphous Titanium Phosphates. *Journal of Non-Crystalline Solids*, **170**, 250-262. https://doi.org/10.1016/0022-3093(94)90054-x

[42] Araújo, A.M.C.F., Freitas, D.F.S., Souza, Y.C.A., Albitres, G.A.V., Garcia, E.E., Cestari, S.P., *et al.* (2024) Building and Evaluating a Green and Multifunctional Composite Based on Poly(Butylene Adipate-Co Terephthalate) with Zirconium Phosphate and Clove Essential Oil. *European Journal of Applied Sciences*, **12**, 353-376. https://doi.org/10.14738/aivp.126.17981

[43] Freitas, D.F.S., Araújo, A.M.C.F., Souza, Y.C.A., Albitres, G.A.V., Garcia, E.E., Cestari, S.P., Miguel, M.A.L. and Mendes, L.C. (2025) Ecofriendly-Multifunctional Composite of Poly(Butylene Adipate-*co*-Terephthalate)/Zirconium Phosphate/Cinnamon Oil. *Nanotechnology, Science and Applications*, **8**, 1-12.

[44] Blümich, B. (2019) Low-Field and Benchtop NMR. *Journal of Magnetic Resonance*, **306**, 27-35. https://doi.org/10.1016/j.jmr.2019.07.030

[45] Patel, J.P. and Hsu, S.L. (2018) Development of Low Field NMR Technique for Analyzing Segmental Mobility of Crosslinked Polymers. *Journal of Polymer Science Part B: Polymer Physics*, **56**, 639-643. https://doi.org/10.1002/polb.24583

[46] Albitres, G.A.V., Araujo Junior, F.P., Freitas, D.F.S., Mariano, D.M., Tavares, M.I.B. and Mendes, L.C. (2022) Nanocellulose: Effect on Thermal, Structural, Molecular Mobility and Rheological Characteristics of Poly(Butylenes Adipate-*co*-Butylene Terephthalate) Nanocomposites. *Materials Sciences and Applications*, **13**, 249-277. https://doi.org/10.4236/msa.2022.134014

[47] Nascimento, C.K.S., Silva, K.D.E., Vitorino, G.B.L., Diniz, A.C.O., Silva, I.D.L., Simões, A.N., *et al.* (2026) Atmospheric Degradation of Pure and Rosemary (*Rosmarinus officinalis* (L.)) Essential Oil-Added Antimicrobial Poly(Butylene Adipate-*co*-Terephthalate) (PBAT) Films. *ACS Omega*, **11**, 43375-43384. https://doi.org/10.1021/acsomega.6c01636

[48] Rusanova-Naydenova, D., Trublet, M., Klysubun, W., Cholsuk, C., Iuga, D., Dupree, R., *et al.* (2022) Synthesis and Structural Characterisation of Solid Titanium(IV) Phosphate Materials by Means of X-Ray Absorption and NMR Spectroscopy. *Dalton Transactions*, **51**, 8192-8207. https://doi.org/10.1039/d2dt00902a

[49] Li, B., You, W., Peng, L., Zhang, C., Huang, X. and Yu, W. (2023) Role of Monomer Sequence in the Crystallization and Rheology of PBAT. *Polymer*, **283**, Article 126228. https://doi.org/10.1016/j.polymer.2023.126228

[50] Moraes Filho, L.E.P.T., Andrade, M.F., Freitas, L.F., Palha, M.d.L.A.P.F. and Vinhas, G.M. (2022) Development and Characterization of Poly(Butylene Adipate-*co*-Terephthalate) (PBAT) Antimicrobial Films with Clove and Cinnamon Essential Oils. *Journal of Food Processing and Preservation*, **46**, e16489. https://doi.org/10.1111/jfpp.16489

[51] Ooi, L.S.M., Li, Y., Kam, S., Wang, H., Wong, E.Y.L. and Ooi, V.E.C. (2006) Antimicrobial Activities of Cinnamon Oil and Cinnamaldehyde from the Chinese Medicinal Herb *Cinnamomum cassia* Blume. *The American Journal of Chinese Medicine*, **34**, 511-522. https://doi.org/10.1142/s0192415x06004041